



Observation of the $\Lambda_b^0 \rightarrow J/\psi \Xi^- K^+$ and $\Xi_b^0 \rightarrow J/\psi \Xi^- \pi^+$ decays

LHCb Collaboration*

CERN, 1211 Geneva 23, Switzerland

Received: 24 January 2025 / Accepted: 26 March 2025
© CERN for the benefit of the LHCb collaboration 2025

Abstract The first observation of the $\Xi_b^0 \rightarrow J/\psi \Xi^- \pi^+$ decay and the most precise measurement of the branching fraction of the $\Lambda_b^0 \rightarrow J/\psi \Xi^- K^+$ decay are reported, using proton-proton collision data from the LHCb experiment collected in 2016–2018 at a centre-of-mass energy of 13 TeV, corresponding to an integrated luminosity of 5.4 fb^{-1} . Using the $\Lambda_b^0 \rightarrow J/\psi \Lambda$ and $\Xi_b^- \rightarrow J/\psi \Xi^-$ decays as normalisation channels, the ratios of branching fractions are measured to be

$$\frac{\mathcal{B}(\Lambda_b^0 \rightarrow J/\psi \Xi^- K^+)}{\mathcal{B}(\Lambda_b^0 \rightarrow J/\psi \Lambda)} = (1.17 \pm 0.14 \pm 0.08) \times 10^{-2},$$
$$\frac{\mathcal{B}(\Xi_b^0 \rightarrow J/\psi \Xi^- \pi^+)}{\mathcal{B}(\Xi_b^- \rightarrow J/\psi \Xi^-)} = (11.9 \pm 1.4 \pm 0.6) \times 10^{-2},$$

where the first uncertainty is statistical and the second systematic.

1 Introduction

The existence of pentaquark states has been predicted since the establishment of the quark model [1, 2]. In 2015 the first pentaquark states were observed by the LHCb experiment in the spectrum of $\Lambda_b^0 \rightarrow J/\psi p K^-$ decays [3].¹ This observation sparked significant interest in the community, leading to various interpretations on the internal structure of these states [4–8]. In the subsequent years, numerous pentaquark states have been discovered in b -hadron decays to final states containing charmonium [9–12]. After the observation of pentaquarks with strangeness $S = 0$ and $S = 1$ in the $J/\psi p$ and $J/\psi \Lambda$ systems, the search for a pentaquark with $S = -2$ in the $J/\psi \Xi^-$ system is the next natural step [13, 14]. In this paper, the foundation for these searches is laid by the observation of the $\Lambda_b^0 \rightarrow J/\psi \Xi^- K^+$ and $\Xi_b^0 \rightarrow J/\psi \Xi^- \pi^+$ decays.

¹ Charge conjugation is implied throughout this paper.

* e-mail: luis.miguel.garcia.martin@cern.ch

Besides the search for exotic states in decay products including a charmonium resonance, the studied decay channels give insights into the dynamics of baryon-meson systems with one or two units of strangeness [15]. Of particular interest are $\bar{K}N$ meson-baryon interactions which are used to describe the $\Lambda(1405)$ resonance using Unitarised Chiral Perturbation Theory [16]. These interactions have been studied using data from $K^- p \rightarrow KN, \pi \Sigma, \pi^0 \Lambda$ inelastic scattering, near threshold production of the $\Lambda(1405)$ resonance [17]. Scattering studies at higher energies — above the $K \Xi$ threshold — are interesting since they are sensitive to next-to-leading order terms of the Chiral Lagrangian [17]. Most of the $\bar{K}N \rightarrow K \Xi$ data come from antikaon-proton scattering, which includes both isospin $I = 0$ and $I = 1$ contributions. In contrast, $K^- p$ scattering, which occurs in the decay process $\Lambda_b^0 \rightarrow J/\psi \Xi^- K^+$, is restricted to $I = 0$ contribution in order to preserve the overall isospin of the decay. Studying this weak process therefore allows the $I = 0$ component to be isolated, thus enhancing our understanding of meson-baryon interactions [18]. In the $\Lambda_b^0 \rightarrow J/\psi \Xi^- K^+$ decay, the direct production of the $\Xi^- K^+$ final state is forbidden in the quark model, and is only reached via a two-step process, as shown in Fig. 1. First, the $\Lambda_b^0 \rightarrow J/\psi \{ \Lambda \eta, p K^-, n \bar{K} \}$ decay proceeds via the weak interaction. Second, the meson-baryon pair produced in the decay scatters into a $\Xi^- K^+$ pair [17].

A measurement of the $m(\Xi^- K^+)$ spectrum in the $\Lambda_b^0 \rightarrow J/\psi \Xi^- K^+$ decay isolates the $I = 0$ contribution, and allows the $I = 0$ and $I = 1$ contributions in previous data [17] to be disentangled. As a consequence, the modelling of meson-baryon interaction above the $\Lambda(1405)$ resonance can be improved.

The $\Xi_b^0 \rightarrow J/\psi \Xi^- \pi^+$ decay has not yet been observed. This decay is expected to receive contributions from $\Xi_b^0 \rightarrow J/\psi \Xi^*(\Xi^- \pi^+)$ processes, where Ξ^* are excited states of the Ξ baryon. The first excitation of the Ξ baryon, the $\Xi(1530)^0$ state, is flavour-symmetric and would be suppressed in the $\Xi_b^0 \rightarrow \Xi(1530)^0$ transition due to the Ξ_b^0 state being flavour-antisymmetric [19]. Measuring the $\Xi_b^0 \rightarrow J/\psi \Xi(1530)^0$ decay rate is a method to quantify

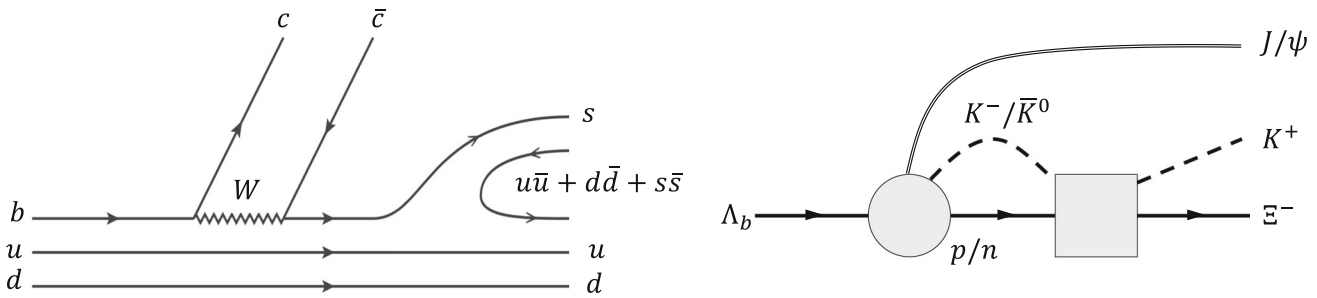


Fig. 1 (Left) Production of a pK^- , $n\bar{K}^0$ or $\Lambda\eta$ pair from the weak decay $\Lambda_b^0 \rightarrow J/\psi \Lambda$ via a hadronisation mechanism. (Right) Final-state interaction of the meson-baryon pair, where the double line denotes the J/ψ meson, solid lines represent baryons and dashed lines denote the

pseudoscalar mesons. The shaded circle and square stand for the production mechanism of the $J/\psi pK^-$ or $J/\psi n\bar{K}^0$, and the meson-baryon scattering matrix, respectively

the mixing of symmetric and antisymmetric flavour states. The $\Xi^-\pi^+$ invariant-mass spectrum in $\Xi_b^0 \rightarrow J/\psi \Xi^-\pi^+$ decays can help explore possible mixing between flavour-symmetric and -antisymmetric contributions. Furthermore, the $\Xi_b^0 \rightarrow J/\psi \Xi^-\pi^+$ channel provides an excellent opportunity to search for charmonium pentaquark states. The first step towards the study of the decay dynamics is to observe these decay channels and analyse their mass spectra. This paper details the first measurement of the $\Xi_b^0 \rightarrow J/\psi \Xi^-\pi^+$ branching fraction and improves the precision of the $\Lambda_b^0 \rightarrow J/\psi \Xi^-K^+$ branching fraction with respect to the latest measurement by the CMS collaboration [20]. The measurements reported in this paper use pp collision data collected by the LHCb experiment in 2016–2018 at a centre-of-mass energy of 13 TeV, corresponding to an integrated luminosity of 5.4 fb^{-1} .

The $\Lambda_b^0 \rightarrow J/\psi \Xi^-K^+$ and $\Xi_b^0 \rightarrow J/\psi \Xi^-\pi^+$ signal channels are reconstructed through the $J/\psi \rightarrow \mu^+\mu^-$, $\Xi^- \rightarrow \Lambda\pi^-$ and $\Lambda \rightarrow p\pi^-$ decays. The $\Lambda_b^0 \rightarrow J/\psi \Lambda$ and $\Xi_b^- \rightarrow J/\psi \Xi^-$ decay modes are used as normalisation channels due to their similar experimental signature. The choice of normalisation channels enables the cancellation of the dependence on b -hadron production rates and minimises systematic uncertainties related to final-state particle reconstruction. The ratios of branching fractions are measured as

$$\frac{\mathcal{B}(\Lambda_b^0 \rightarrow J/\psi \Xi^-K^+)}{\mathcal{B}(\Lambda_b^0 \rightarrow J/\psi \Lambda)} = \frac{N(\Lambda_b^0 \rightarrow J/\psi \Xi^-K^+)}{N(\Lambda_b^0 \rightarrow J/\psi \Lambda)} \cdot \frac{\varepsilon(\Lambda_b^0 \rightarrow J/\psi \Lambda)}{\varepsilon(\Lambda_b^0 \rightarrow J/\psi \Xi^-K^+)} \cdot \mathcal{B}(\Xi^- \rightarrow \Lambda\pi^-), \quad (1)$$

$$\frac{\mathcal{B}(\Xi_b^0 \rightarrow J/\psi \Xi^-\pi^+)}{\mathcal{B}(\Xi_b^- \rightarrow J/\psi \Xi^-)} = \frac{N(\Xi_b^0 \rightarrow J/\psi \Xi^-\pi^+)}{N(\Xi_b^- \rightarrow J/\psi \Xi^-)} \cdot \frac{\varepsilon(\Xi_b^- \rightarrow J/\psi \Xi^-)}{\varepsilon(\Xi_b^0 \rightarrow J/\psi \Xi^-\pi^+)}, \quad (2)$$

where \mathcal{B} is the branching fraction, N is the number of observed decays and ε is the total efficiency for the corresponding decay. An event selection is developed using simulated samples to optimise the search sensitivity. Correct estimation of the efficiencies relies on the accurate modelling of the physics processes and detector response in the simulation. The normalisation channels are used to correct for inaccuracies in the simulation for observables with a significant disagreement between simulation and data. After the selection is completed, the signal and normalisation yields are obtained from fits to the invariant-mass distributions of candidates in the selected data. In addition, the background-subtracted invariant-mass distributions of the Ξ^-K^+ , $J/\psi K^+$ and $J/\psi \Xi^-$ pairs for the $\Lambda_b^0 \rightarrow J/\psi \Xi^-K^+$ channel, and the $\Xi^-\pi^+$, $J/\psi \pi^+$ and $J/\psi \Xi^-$ pairs for the $\Xi_b^0 \rightarrow J/\psi \Xi^-\pi^+$ channel are investigated. The background-subtracted samples are obtained using the `sPlot` technique [21, 22], a statistical method that separates signal and background distributions using event-by-event weights derived from a fit to discriminating variables. The b -baryon invariant-mass is chosen as discriminant variable. The invariant-mass signal regions were not examined until the full procedure had been finalised.

2 Detector and simulation

The LHCb detector [23, 24] is a single-arm forward spectrometer covering the pseudorapidity range $2 < \eta < 5$, designed for the study of particles containing b or c quarks. The detector used to collect data in 2015–2018 (Run 2) includes a high-precision tracking system consisting of a silicon-strip vertex detector (VELO) surrounding the pp interaction region, a large-area silicon-strip detector, the Tracker Turicensis (TT), located upstream of a dipole magnet with a bending power of about 4 T m, and three stations of silicon-strip detectors, straw drift tubes (T-stations) placed downstream of the magnet. The tracking system provides a

measurement of the momentum, p , of charged particles with a relative uncertainty that varies from 0.5% at low momentum to 1.0% at 200 GeV/ c . The minimum distance of a track to a primary pp collision vertex (PV), the impact parameter (IP), is measured with a resolution of $(15 + 29/p_T) \mu\text{m}$, where p_T is the component of the momentum transverse to the beam, in GeV/ c . Different types of charged hadrons are distinguished using information from two ring-imaging Cherenkov detectors. Muons are identified by a system composed of alternating layers of iron and multiwire proportional chambers. The online event selection [25] is performed by a trigger which consists of a hardware stage, based on information from the calorimeter and muon systems, followed by two software stages, which apply a partial and full event reconstruction, respectively. At the hardware trigger stage, events are required to have muon or dimuon candidates with high p_T . The software trigger requires a two-track secondary vertex with a significant displacement from any PV. At least one charged particle must have $p_T > 1.6 \text{ GeV}/c$ and be inconsistent with originating from a PV.

Simulated samples are used to develop the selection strategy, compute the efficiencies and model the shape of the invariant-mass distribution of the signal decays. In the simulation, pp collisions are generated using PYTHIA [26] with a specific LHCb configuration [27]. Decays of unstable particles are described by EVTGEN [28], in which final-state radiation is generated using PHOTOS [29]. The interaction of the generated particles with the detector, and its response, are implemented using the GEANT4 toolkit [30, 31] as described in Ref. [32]. For each generated signal decay the underlying pp interaction is reused multiple times [33].

3 Candidate selection and efficiencies

The selection begins by identifying well-reconstructed tracks that do not originate from any PV. Candidates with two oppositely charged tracks identified as muons are selected. Each muon candidate must fulfil $p_T > 250 \text{ MeV}/c$ requirement. Dimuon pairs originating from a common vertex that is significantly displaced from any PV are combined to form J/ψ candidates. The dimuon pair must have a reconstructed invariant mass compatible with the nominal mass of the J/ψ meson. Oppositely charged tracks assigned to proton and pion mass hypotheses are combined to form Λ candidates. The $p\pi^-$ invariant mass is required to be within $\pm 10 \text{ MeV}/c^2$ of the known Λ mass [34]. The Λ candidates are further combined with another particle, assigned the pion mass hypothesis, to reconstruct Ξ^- candidates. The selected $\Lambda\pi^-$ pairs must have a p_T larger than $250 \text{ MeV}/c^2$ and an invariant mass within $\pm 20 \text{ MeV}/c^2$ of the known Ξ^- mass [34]. For reference, the mass resolution of the Λ and Ξ^- signals are about $1.7 \text{ MeV}/c^2$ and $3.0 \text{ MeV}/c^2$, respectively. Given the relatively

large lifetime of the Λ and Ξ^- baryons, most of these candidates decay downstream of the VELO, but before reaching the TT. Tracks that are reconstructed only from hits in the TT and the T-stations are called downstream tracks. Tracks that are reconstructed using hits in the VELO, the T-stations, and optionally in the TT, are called long tracks. Long tracks profit from the superior resolution of the vertex detector and have better mass, momentum and vertex position resolution than downstream tracks. The considered $\Lambda \rightarrow p\pi^-$ candidates can be reconstructed from two long tracks or two downstream tracks. Similarly, the $\Xi^- \rightarrow \Lambda\pi^-$ decay is reconstructed using three main categories of track-type combinations: (i) both Λ and π^- candidates reconstructed only from long tracks, (ii) both Λ and π^- candidates reconstructed only from downstream tracks, and (iii) the Λ candidate reconstructed from two downstream tracks and the accompanying π^- candidate reconstructed as a long track. The Λ_b^0 (Ξ_b^0) signal candidate is formed by combining the J/ψ and Ξ^- candidates with a long track identified as a K^+ (π^+) candidate with $p_T > 250 \text{ MeV}/c$. Similarly, J/ψ and Λ (Ξ^-) candidates are combined to form Λ_b^0 (Ξ_b^-) candidates corresponding to the normalisation channel decay. Both Λ and Ξ^- candidates are required to have a decay time greater than 2 ps to reject background from short-lived particles. The Λ_b^0 (Ξ_b) decay vertices must have a good fit quality and be significantly displaced from any PV. A kinematic fit [35] is performed to improve the b -hadron mass resolution by constraining the mass hypothesis of the J/ψ , Ξ^- and Λ candidates to their known masses [34] and requiring the b hadron to originate from its associated PV.² Candidates with a poor quality of the kinematic fit or a Λ_b^0 (Ξ_b) invariant mass from the kinematic fit outside the range [5360, 5900] ([5700, 6100]) MeV/ c^2 are rejected.

The final step of the selection for the four decays channels is to apply a boosted decision tree (BDT) [36, 37] classifier implemented using the XGBoost toolkit [38]. Each classifier is trained to distinguish between the specific b -hadron decay and combinatorial background. Simulation samples are used as a proxy for the specific b -hadron decays. The background samples are taken from the high invariant-mass sideband [5700, 5900] ([5900, 6100]) MeV/ c^2 of selected Λ_b^0 (Ξ_b) data candidates. The BDT classifier exploits the discriminating power of the IP of the π^- meson from the Ξ^- decay, and Λ decay products with respect to any PV; the difference in the vertex-fit χ^2 of a given PV reconstructed with and without the b -hadron and the muons; the χ^2 of the kinematic fit; the decay time of the b hadron and Ξ^- baryon; and the p_T of the Ξ^- candidate. Most of the training variables are common between the signal and normalisation channels, with the exception of variables associated with the Ξ^- can-

² The associated PV is defined as the PV that fits best to the flight direction of the b -hadron candidate.

didate that are excluded when analysing the $\Lambda_b^0 \rightarrow J/\psi \Lambda$ mode. The BDT working point is chosen by maximising a figure of merit [39], defined as $\varepsilon_s/(\sqrt{B}+2.5)$, where ε_s is the efficiency of the requirement on the BDT output for simulated signal events, and B is the background yield in a region within 3 sigmas around the nominal b -hadron mass, extrapolated from the high invariant-mass sideband. The BDT classifier removes more than 99% of the background while retaining approximately 70% of the signal in the four considered decay modes. After the described selection, more than one candidates are selected per pp in less than 1% of the events. In this cases, the candidate with the highest BDT score is kept.

The total efficiency is calculated as the product of efficiencies of detector acceptance, reconstruction, and selection. Accurate simulation is crucial to determine such selection efficiencies, and also to train the BDT algorithms and model the signal mass shapes. Discrepancies between data and simulation are observed and corrected for in the b -baryon p_T , the χ^2 of the kinematic fit, angular and two-body invariant-mass distributions, and particle identification and tracking efficiencies. The corrections are derived sequentially, *i.e.* adjusting the distribution for one variable at a time. Potential correlations between variables are accounted for by deriving each correction factor on top of previous ones. The particle identification efficiencies for the different particle species are measured using charm hadron data samples reconstructed without the use of PID information [40]. The correction factors for the tracking efficiencies are derived from a dedicated data sample of $J/\psi \rightarrow \mu^+ \mu^-$ decays [41]. The correction factors for b -baryon p_T and the χ^2 of the kinematic fit are extracted from a comparison of $\Lambda_b^0 \rightarrow J/\psi \Lambda$ and $\Xi_b^- \rightarrow J/\psi \Xi^-$ decays between background-subtracted data and simulated samples and applied to both signal and normalisation channels. The angular distribution could differ between the signal and normalisation channels, and thus the above correction factors are derived independently for each of the four channels. The decay dynamics of the signal channels are also corrected for the $m(J/\psi \Xi^-)$ and $m(\Xi^- K^+)$, or $m(\Xi^- \pi^+)$, distributions. The variables corrected are those that demonstrated a significant correlation with the efficiency. These correction factors are derived from the $\Lambda_b^0 \rightarrow J/\psi \Xi^- K^+$ and $\Xi_b^0 \rightarrow J/\psi \Xi^- \pi^+$ signal channels. No significant correlation is observed between the discriminant variable used for the background-subtraction method, the b -hadron invariant mass improved by the kinematic fit, and the corrected variables. After applying the correction, a good agreement is observed between the background-subtracted data and the simulation on all variables used for the selection, including the BDT response. The ratios of efficiencies between the Λ_b^0 and Ξ_b modes, required in Eqs. (1) and (2), are determined to be

$$\frac{\varepsilon(\Lambda_b^0 \rightarrow J/\psi \Lambda)}{\varepsilon(\Lambda_b^0 \rightarrow J/\psi \Xi^- K^+)} = 5.30 \pm 0.05,$$

$$\frac{\varepsilon(\Xi_b^- \rightarrow J/\psi \Xi^-)}{\varepsilon(\Xi_b^0 \rightarrow J/\psi \Xi^- \pi^+)} = 1.64 \pm 0.02,$$

where the uncertainty is due to the limited size of the simulation samples. This uncertainty is propagated to the branching fraction ratios as a source of systematic uncertainty in Sect. 5.

4 Signal yield determination

An extended unbinned maximum-likelihood fit is performed to the b -hadron invariant-mass spectrum of the $\Lambda_b^0 \rightarrow J/\psi \Xi^- K^+$ and $\Lambda_b^0 \rightarrow J/\psi \Lambda$ modes in the range [5360, 5900] MeV/ c^2 . An analogous, independent fit is performed to the $\Xi_b^0 \rightarrow J/\psi \Xi^- \pi^+$ and $\Xi_b^- \rightarrow J/\psi \Xi^-$ candidates in the range [5700, 6100] MeV/ c^2 . The invariant-mass shape of the $\Lambda_b^0 \rightarrow J/\psi \Lambda$ decay mode is modelled by a Hypatia function [42]. The signal for the other three channels is modelled by the sum of two Crystal Ball functions [43] with common mean and width. The tail parameters for both signal models, Hypatia and two Crystal Ball functions, are fixed according to simulation. The shape of the invariant-mass distribution of the combinatorial background is modelled by an exponential function with a slope varying freely in the fit. Non-negligible contribution from decays of other b -hadrons is only observed in the $\Lambda_b^0 \rightarrow J/\psi \Lambda$ channel. The two main background sources are $B^0 \rightarrow J/\psi K_S^0$ and $\Xi_b^- \rightarrow J/\psi \Xi^-$ decays. The $B^0 \rightarrow J/\psi K_S^0$ decay can be misidentified as a $\Lambda_b^0 \rightarrow J/\psi \Lambda$ candidate if the proton hypothesis is wrongly assigned to the π^+ meson in the K_S^0 decay. Additionally, missing the pion from the $\Xi^- \rightarrow \Lambda \pi^-$ decay leads to a $\Xi_b^- \rightarrow J/\psi \Xi^-$ decay that is partially reconstructed as a $\Lambda_b^0 \rightarrow J/\psi \Lambda$ candidate. The invariant-mass shapes of the misidentified $B^0 \rightarrow J/\psi K_S^0$ and partially reconstructed $\Xi_b^- \rightarrow J/\psi \Xi^-$ backgrounds are derived from simulation in terms of a nonparametric probability density function using a kernel density estimation method [44, 45] and a Johnson S_U function [46], respectively. The shapes of these functions are fixed from simulation.

Figures 2 and 3 show the result of the fits to the invariant-mass spectra for Λ_b^0 and Ξ_b candidates, respectively.

The Λ_b^0 invariant-mass fits determine yields of 84 ± 10 $\Lambda_b^0 \rightarrow J/\psi \Xi^- K^+$ signal and 39390 ± 220 $\Lambda_b^0 \rightarrow J/\psi \Lambda$ normalisation decays. The Ξ_b invariant-mass fits determine yields of 107 ± 12 $\Xi_b^0 \rightarrow J/\psi \Xi^- \pi^+$ signal and 1450 ± 40 $\Xi_b^- \rightarrow J/\psi \Xi^-$ normalisation decays. Both signal modes are observed with a significance greater than 10σ using the Wilk's theorem [47].

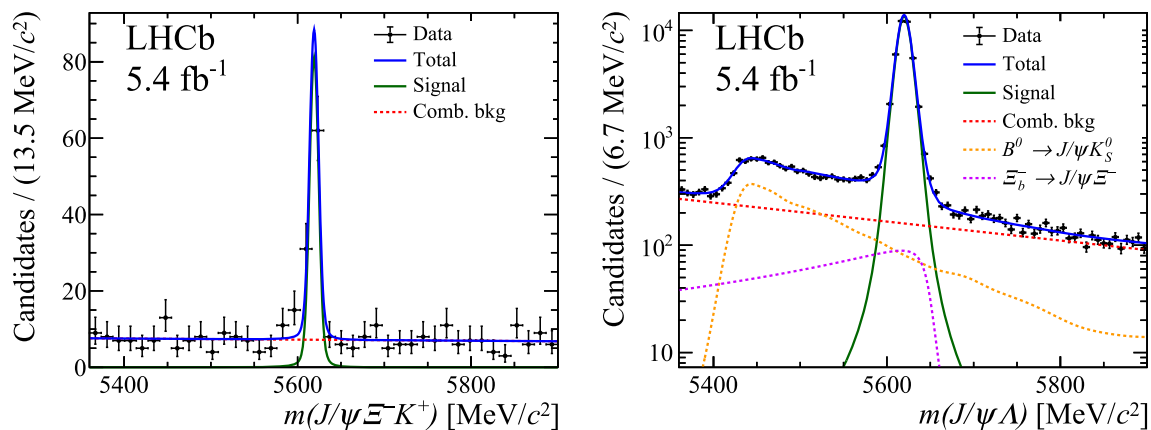


Fig. 2 Invariant-mass distribution of selected (left) $\Lambda_b^0 \rightarrow J/\psi \Xi^- K^+$ and (right) $\Lambda_b^0 \rightarrow J/\psi \Lambda$ candidates with the result of the fit also shown

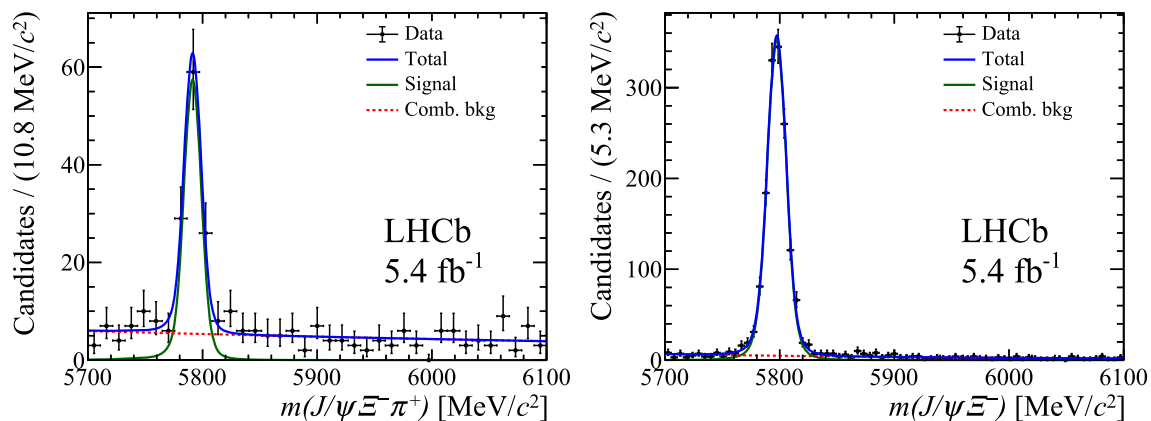


Fig. 3 Invariant-mass distribution of selected (left) $\Xi_b^0 \rightarrow J/\psi \Xi^- \pi^+$ and (right) $\Xi_b^- \rightarrow J/\psi \Xi^-$ candidates with the result of the fit also shown

5 Systematic uncertainties

Systematic uncertainties on the $\mathcal{B}(\Lambda_b^0 \rightarrow J/\psi \Xi^- K^+)/\mathcal{B}(\Lambda_b^0 \rightarrow J/\psi \Lambda)$ and $\mathcal{B}(\Xi_b^0 \rightarrow J/\psi \Xi^- \pi^+)/\mathcal{B}(\Xi_b^- \rightarrow J/\psi \Xi^-)$ measurements arise from several sources. A summary of the uncertainties is provided in Table 1.

The systematic effect due to the choice of the invariant-mass fit model is assessed by means of pseudoexperiments wherein the invariant-mass distribution is generated with an alternative model and fitted using the baseline model. The alternative model replaces the two Crystal Ball functions by an Hypatia function (or vice versa for the $\Lambda_b^0 \rightarrow J/\psi \Lambda$ case) for the signal. The physical backgrounds in the $\Lambda_b^0 \rightarrow J/\psi \Lambda$ channel are both modelled with a single Crystal Ball function in the alternative model.

The uncertainty on the selection efficiencies originating from the limited size of the simulated samples is propagated to the branching fraction and considered as a systematic uncertainty.

The corrections applied to the simulation to improve the agreement with data are obtained with an uncertainty. The effect of this limited precision is assessed by varying the cor-

rections within their uncertainty and recomputing the efficiencies 100 times. The standard deviation of the efficiency variation is assigned as a systematic uncertainty. As the corrections used for the $\Xi_b^0 \rightarrow J/\psi \Xi^- \pi^+$ and $\Xi_b^- \rightarrow J/\psi \Xi^-$ channels are almost the same, a good level of cancellation is obtained. On the other hand, some of the corrections applied to the $\Lambda_b^0 \rightarrow J/\psi \Xi^- K^+$ and $\Lambda_b^0 \rightarrow J/\psi \Lambda$ channels are different and, therefore they do not cancel in the ratio.

The χ^2 distribution of each kinematic fit is corrected using the normalisation channels as calibration samples. While the normalisation decay topology is similar, it is not identical to the signal decay. Alternative corrections for the simulations are derived by swapping the calibration channel, *i.e.* using the $\Lambda_b^0 \rightarrow J/\psi \Lambda$ channel for $\Xi_b^0 \rightarrow J/\psi \Xi^- \pi^+$ corrections and the $\Xi_b^- \rightarrow J/\psi \Xi^-$ channel for $\Lambda_b^0 \rightarrow J/\psi \Xi^- K^+$ corrections. The variation in the efficiency is assigned as the systematic uncertainty.

After applying the baseline corrections to the simulation, some level of mismodelling remains in variables not used directly in the selection. The effect of this mismodelling is assessed by recomputing the efficiencies after correcting the

Table 1 Summary of relative systematic uncertainties (in percent) for the measured ratio of branching fractions. The individual sources are described in the text. The total relative uncertainty is determined by adding the individual sources in quadrature

Source	$\frac{\mathcal{B}(\Lambda_b^0 \rightarrow J/\psi \mathcal{E}^- K^+)}{\mathcal{B}(\Lambda_b^0 \rightarrow J/\psi \Lambda)}$ [%]	$\frac{\mathcal{B}(\mathcal{E}_b^0 \rightarrow J/\psi \mathcal{E}^- \pi^+)}{\mathcal{B}(\mathcal{E}_b^- \rightarrow J/\psi \mathcal{E}^-)}$ [%]
Fit model	1.9	1.3
Size of the simulated samples	0.9	1.2
Corrections to simulation	3.4	1.1
Alternative corrections	1.1	1.2
Additional corrections	1.9	1.0
Tracking efficiency	1.5	1.4
Truth matching	1.3	1.2
Phase-space model	4.5	3.8
Total	6.7	5.0

additional distributions and the difference with respect to the baseline efficiency is added as a systematic uncertainty.

The signal channels feature a prompt hadron without a counterpart in the normalisation channel. An additional uncertainty on tracking efficiency of 1.4% for pions and 1.1% for kaons is added which accounts for hadronic interactions that do not cancel in the efficiency ratio. Additionally, the pion from the $\mathcal{E}^- \rightarrow \Lambda \pi^-$ decay in the $\Lambda_b^0 \rightarrow J/\psi \mathcal{E}^- K^+$ signal channel does not have a counterpart in the $\Lambda_b^0 \rightarrow J/\psi \Lambda$ normalisation channel. This pion can be reconstructed as a downstream track, whose reconstruction efficiency is controlled only at the 1% level [48]. The 1% precision is also added as systematic uncertainty to the Λ_b^0 result.

Efficiencies are determined from simulated samples and rely on an accurate match between generated and reconstructed decays. In some cases, this so-called truth matching can fail if the fraction of hits associated between the reconstructed track and the generated particle does not reach a minimum threshold. The effect of such potential incorrect matching is evaluated by recomputing the efficiencies with an alternative method that does not rely on truth matching. Instead, the number of signal events after the selection, required to compute the efficiency, is determined by an invariant-mass fit of the b -hadron spectrum, similar to the approach used for data. The difference in efficiency derived from the baseline and the alternative method is assigned as the systematic uncertainty.

Lastly, inaccuracies in the phase-space model used for signal simulation could affect the derived efficiency. The decay dynamics and angular distributions are corrected using the signal channels. The effect of the limited precision on the derived corrections is assessed by recalculating 100 times the efficiencies after varying the correction factors within their statistical uncertainty. The standard deviation is assigned as the systematic uncertainty.

The systematic uncertainties described in the section above are considered to be uncorrelated and added in quadrature.

6 Results

By combining the signal and normalisation yields from the invariant-mass fits with the selection efficiency ratios as shown in Eqs. (1) and (2), and using the known branching fraction $\mathcal{B}(\mathcal{E}^- \rightarrow \Lambda \pi^-) = 0.99887 \pm 0.00035$ [34], the following results are obtained:

$$\frac{\mathcal{B}(\Lambda_b^0 \rightarrow J/\psi \mathcal{E}^- K^+)}{\mathcal{B}(\Lambda_b^0 \rightarrow J/\psi \Lambda)} = (1.17 \pm 0.14 \pm 0.08) \times 10^{-2},$$

$$\frac{\mathcal{B}(\mathcal{E}_b^0 \rightarrow J/\psi \mathcal{E}^- \pi^+)}{\mathcal{B}(\mathcal{E}_b^- \rightarrow J/\psi \mathcal{E}^-)} = (11.9 \pm 1.4 \pm 0.6) \times 10^{-2},$$

where the first uncertainty is statistical, and the second is systematic. It is possible to convert the $\mathcal{B}(\Lambda_b^0 \rightarrow J/\psi \mathcal{E}^- K^+)/\mathcal{B}(\Lambda_b^0 \rightarrow J/\psi \Lambda)$ ratio to the $\mathcal{B}(\Lambda_b^0 \rightarrow J/\psi \mathcal{E}^- K^+)/\mathcal{B}(\Lambda_b^0 \rightarrow \psi(2S)\Lambda)$ ratio using the world average of $\mathcal{B}(\Lambda_b^0 \rightarrow \psi(2S)\Lambda)/\mathcal{B}(\Lambda_b^0 \rightarrow J/\psi \Lambda) = 0.508 \pm 0.023$ [34] and compare it with the CMS result [20]:

$$\left. \frac{\mathcal{B}(\Lambda_b^0 \rightarrow J/\psi \mathcal{E}^- K^+)}{\mathcal{B}(\Lambda_b^0 \rightarrow \psi(2S)\Lambda)} \right|_{\text{CMS}} = (3.4 \pm 1.2) \times 10^{-2},$$

$$\left. \frac{\mathcal{B}(\Lambda_b^0 \rightarrow J/\psi \mathcal{E}^- K^+)}{\mathcal{B}(\Lambda_b^0 \rightarrow \psi(2S)\Lambda)} \right|_{\text{LHCb}} = (2.3 \pm 0.3) \times 10^{-2}.$$

The LHCb result reported in this paper is compatible with the one obtained by CMS and improves the precision by a factor of 4.

The branching fraction of the signal channels is obtained from the measured ratios using the known branching fractions of the normalisation channels. The values $\mathcal{B}(\Lambda_b^0 \rightarrow J/\psi \Lambda) = (3.36 \pm 1.11) \times 10^{-4}$ and $\mathcal{B}(\mathcal{E}_b^- \rightarrow J/\psi \mathcal{E}^-) = (5.4 \pm 2.4) \times 10^{-4}$ from Ref. [49]

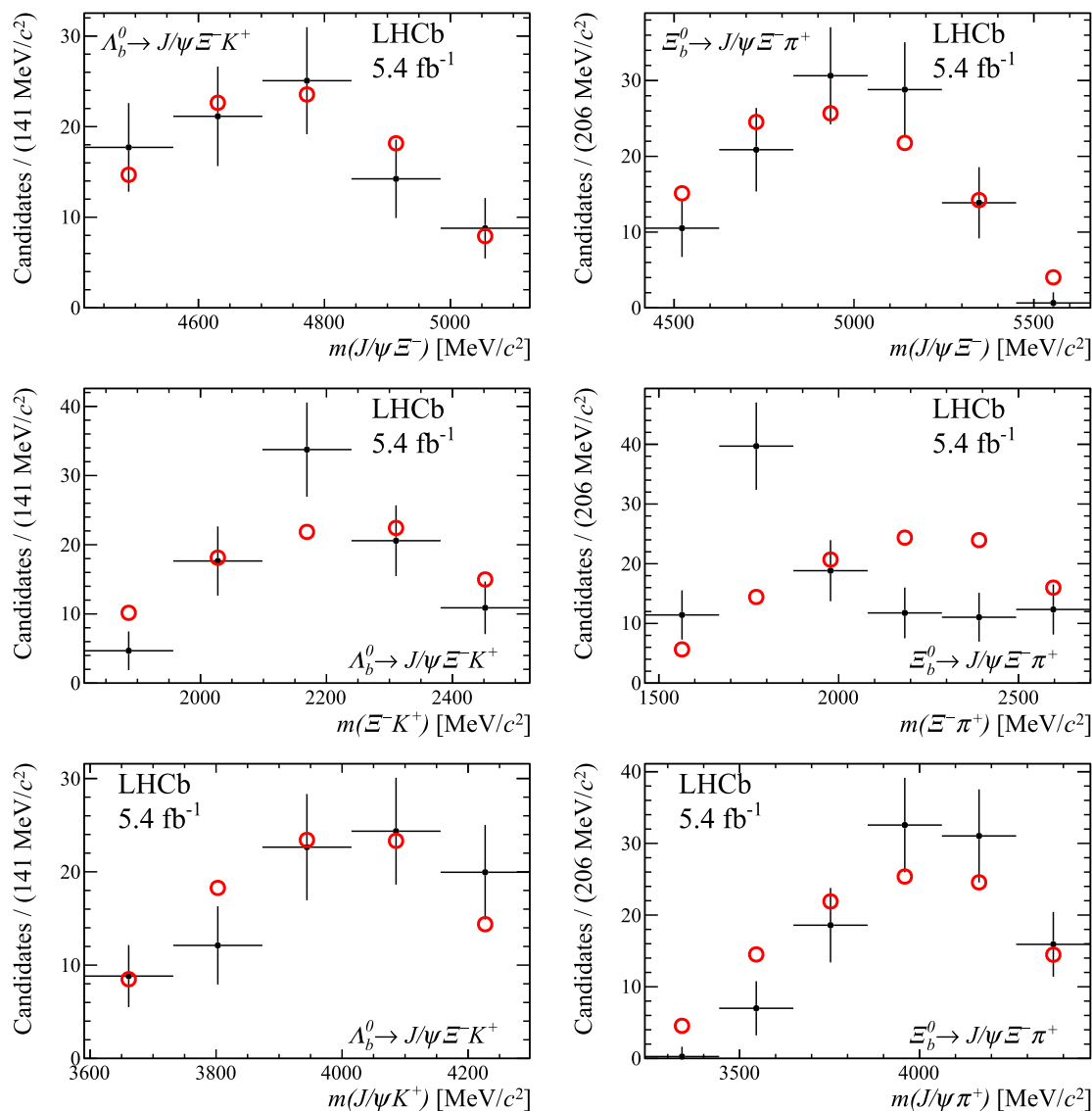


Fig. 4 Invariant-mass distribution of the (top) $J/\psi \Xi^-$, (centre) $\Xi^- K^+$ or $\Xi^- \pi^+$ and (bottom) $J/\psi K^+$ or $J/\psi \pi^+$ systems for the (left) $\Lambda_b^0 \rightarrow J/\psi \Xi^- K^+$ and (right) $\Xi_b^0 \rightarrow J/\psi \Xi^- \pi^+$ decays. The (black)

background-subtracted data is compared to the (red) phase-space simulation including all weights except those for the helicity angles and two-body invariant-mass variables

are used. The signal branching fractions are determined to be:

$$B(\Lambda_b^0 \rightarrow J/\psi \Xi^- K^+) = (3.93 \pm 0.47 \pm 0.27 \pm 1.30) \times 10^{-6},$$

$$B(\Xi_b^0 \rightarrow J/\psi \Xi^- \pi^+) = (6.42 \pm 0.76 \pm 0.32 \pm 2.86) \times 10^{-5},$$

where the first uncertainty is statistical, the second is systematic and the third is due to the external value of the normalisation branching fraction.

The background-subtracted distributions of $m(J/\psi \Xi^-)$, $m(\Xi^- K^+)$ and $m(\Xi^- \pi^+)$ are shown in Fig. 4 and are compared with the phase-space simulation. From this comparison, the only data-simulation disagreement that could point towards a resonance appears in the $m(\Xi^- \pi^+)$ range [1670, 1850] MeV/c² for $\Xi_b^0 \rightarrow J/\psi \Xi^- \pi^+$ candidates. Two resonances, $\Xi(1690)$ and $\Xi(1820)$, with invariant-mass in this range are found in the literature. While the $\Xi(1690)$ resonance is observed to mainly decay to $\Xi^- \pi^+$, the $\Xi(1820)$ resonance is expected to primarily decay to $\Lambda \bar{K}$. Consequently, the decay channel $\Xi_b^0 \rightarrow J/\psi \Xi^- \pi^+$ is more likely to receive contributions from the $\Xi_b^0 \rightarrow J/\psi \Xi(1690)$ tran-

sition. However, no significant evidence supporting this hypothesis is observed in the current measurement. Larger data samples are needed to perform a quantitative study, which is left for the future.

7 Conclusions

In summary, a sample of pp collision data corresponding to an integrated luminosity of 5.4 fb^{-1} is used to measure the $\mathcal{B}(\Lambda_b^0 \rightarrow J/\psi \mathcal{E}^- K^+)/\mathcal{B}(\Lambda_b^0 \rightarrow J/\psi \Lambda)$ and $\mathcal{B}(\Xi_b^0 \rightarrow J/\psi \mathcal{E}^- \pi^+)/\mathcal{B}(\Xi_b^0 \rightarrow J/\psi \mathcal{E}^-)$ ratios. The $\mathcal{B}(\Lambda_b^0 \rightarrow J/\psi \mathcal{E}^- K^+)/\mathcal{B}(\Lambda_b^0 \rightarrow J/\psi \Lambda)$ result is compatible with the CMS measurement and improves its precision by a factor of four. The $\Xi_b^0 \rightarrow J/\psi \mathcal{E}^- \pi^+$ decay is observed for the first time. The branching fraction of the $\Lambda_b^0 \rightarrow J/\psi \mathcal{E}^- K^+$ and $\Xi_b^0 \rightarrow J/\psi \mathcal{E}^- \pi^+$ decays are measured using the known branching fraction of the normalisation channels. This analysis paves the way for future amplitude analysis using larger data sets that will be collected by the upgraded LHCb experiment.

Acknowledgements We express our gratitude to our colleagues in the CERN accelerator departments for the excellent performance of the LHC. We thank the technical and administrative staff at the LHCb institutes. We acknowledge support from CERN and from the national agencies: ARC and ARDC (Australia); CAPES, CNPq, FAPERJ and FINEP (Brazil); MOST and NSFC (China); CNRS/IN2P3 (France); BMBF, DFG and MPG (Germany); INFN (Italy); NWO (Netherlands); MNiSW and NCN (Poland); MCID/IFA (Romania); MICIU and AEI (Spain); SNSF and SER (Switzerland); NASU (Ukraine); STFC (United Kingdom); DOE NP and NSF (USA). We acknowledge the computing resources that are provided by CERN, IN2P3 (France), KIT and DESY (Germany), INFN (Italy), SURF (Netherlands), PIC (Spain), GridPP (United Kingdom), CSCS (Switzerland), IFIN-HH (Romania), CBPF (Brazil), and Polish WLCG (Poland). We are indebted to the communities behind the multiple open-source software packages on which we depend. Individual groups or members have received support from Key Research Program of Frontier Sciences of CAS, CAS PIFI, CAS CCEPP, Fundamental Research Funds for the Central Universities, and Sci. & Tech. Program of Guangzhou (China); Minciencias (Colombia); EPLANET, Marie Skłodowska-Curie Actions, ERC and NextGenerationEU (European Union); A*MIDEX, ANR, IPhU and Labex P2IO, and Région Auvergne-Rhône-Alpes (France); AvH Foundation (Germany); ICSC (Italy); Severo Ochoa and María de Maeztu Units of Excellence, GVA, XuntaGal, GENCAT, InTalent-Inditex and Prog. Atracción Talento CM (Spain); SRC (Sweden); the Leverhulme Trust, the Royal Society and UKRI (United Kingdom).

Data Availability Statement My manuscript has associated data. [Authors' comment: The LHCb experiment has agreed to the CERN open data policy that is summarized in <https://opendata.cern.ch/docs/about>. In particular, Level 1 data associated with this publication are made available on the CERN document server at <https://cds.cern.ch/record/2922172>. These data contain material related to the paper that allows a reinterpretation of the results in the context of new theoretical models. Level 3 data are also available from the CERN open data portal, but due to the large amount of data, only the Run1 dataset has been made public up to now.]

Code Availability Statement Code/software will be made available on reasonable request [Authors' comment: Software/Code that is associated with this publication and that is publicly available is referenced within the publication content. Specific analysis software/code used to produce the results shown in the publication is preserved within the LHCb collaboration internally and can be provided on reasonable request, provided it doesn't contain information that can be associated with unpublished results.]

Open Access This article is licensed under a Creative Commons Attribution 4.0 International License, which permits use, sharing, adaptation, distribution and reproduction in any medium or format, as long as you give appropriate credit to the original author(s) and the source, provide a link to the Creative Commons licence, and indicate if changes were made. The images or other third party material in this article are included in the article's Creative Commons licence, unless indicated otherwise in a credit line to the material. If material is not included in the article's Creative Commons licence and your intended use is not permitted by statutory regulation or exceeds the permitted use, you will need to obtain permission directly from the copyright holder. To view a copy of this licence, visit <http://creativecommons.org/licenses/by/4.0/>. Funded by SCOAP³.

References

1. M. Gell-Mann, A schematic model of baryons and mesons. *Phys. Lett.* **8**, 214 (1964). [https://doi.org/10.1016/S0031-9163\(64\)92001-3](https://doi.org/10.1016/S0031-9163(64)92001-3)
2. G. Zweig, An SU_3 model for strong interaction symmetry and its breaking. Version 1 CERN-TH-401, CERN, Geneva (1964). <http://cds.cern.ch/record/352337>
3. LHCb Collaboration, R. Aaij et al., Observation of $J/\psi p$ resonances consistent with pentaquark states in $\Lambda_b^0 \rightarrow J/\psi K^- p$ decays. *Phys. Rev. Lett.* **115**, 072001 (2015). <https://doi.org/10.1103/PhysRevLett.115.072001>. [arXiv:1507.03414](https://arxiv.org/abs/1507.03414)
4. M.-L. Du et al., Interpretation of the LHCb P_c states as hadronic molecules and hints of a narrow $P_c(4380)$. *Phys. Rev. Lett.* **124**, 072001 (2020). <https://doi.org/10.1103/PhysRevLett.124.072001>. [arXiv:1910.11846](https://arxiv.org/abs/1910.11846)
5. L. Roca, J. Nieves, E. Oset, LHCb pentaquark as a $\bar{D}^* \Sigma_c - \bar{D}^* \Sigma_c^*$ molecular state. *Phys. Rev. D* **92**, 094003 (2015). <https://doi.org/10.1103/PhysRevD.92.094003>. [arXiv:1507.04249](https://arxiv.org/abs/1507.04249)
6. S.X. Nakamura, $P_c(4312)^+$, $P_c(4380)^+$, and $P_c(4457)^+$ as double triangle cusps. *Phys. Rev. D* **103**, 111503 (2021). <https://doi.org/10.1103/PhysRevD.103.L111503>. [arXiv:2103.06817](https://arxiv.org/abs/2103.06817)
7. M.I. Eides, V.Y. Petrov, M.V. Polyakov, Pentaquarks with hidden charm as hadroquarkonia. *Eur. Phys. J. C* **78**, 36 (2018). <https://doi.org/10.1140/epjc/s10052-018-5530-9>. [arXiv:1709.09523](https://arxiv.org/abs/1709.09523)
8. E. Santopinto, A. Giachino, Compact pentaquark structures. *Phys. Rev. D* **96**, 014014 (2017). <https://doi.org/10.1103/PhysRevD.96.014014>. [arXiv:1604.03769](https://arxiv.org/abs/1604.03769)
9. LHCb Collaboration, R. Aaij et al., Observation of a narrow pentaquark state, $P_c(4312)^+$, and of two-peak structure of the $P_c(4450)^+$. *Phys. Rev. Lett.* **122**, 222001 (2019). <https://doi.org/10.1103/PhysRevLett.122.222001>. [arXiv:1904.03947](https://arxiv.org/abs/1904.03947)
10. LHCb Collaboration, R. Aaij et al., Evidence of a $J/\psi \Lambda$ structure and observation of excited Ξ_c^0 states in the $\Xi_b^- \rightarrow J/\psi \Lambda K^-$ decay. *Sci. Bull.* **66**, 1278 (2021). <https://doi.org/10.1016/j.scib.2021.02.030>. [arXiv:2012.10380](https://arxiv.org/abs/2012.10380)
11. LHCb Collaboration, R. Aaij et al., Observation of a $J/\psi \Lambda$ resonance consistent with a strange pentaquark candidate in $B^- \rightarrow J/\psi \Lambda \bar{p}$ decays. *Phys. Rev. Lett.* **131**, 031901 (2023). <https://doi.org/10.1103/PhysRevLett.131.031901>. [arXiv:2210.10346](https://arxiv.org/abs/2210.10346)

12. LHCb Collaboration, R. Aaij et al., Evidence for a new structure in the $J/\psi\phi$ and $J/\psi\omega$ systems in $B_s^0 \rightarrow J/\psi\phi\pi^+\pi^-$ decays. *Phys. Rev. Lett.* **128**, 062001 (2022). <https://doi.org/10.1103/PhysRevLett.128.062001>. arXiv:2108.04720
13. F.-L. Wang, X.-D. Yang, R. Chen, X. Liu, Hidden-charm pentaquarks with triple strangeness due to the $\Omega_c^* \bar{D}^*$ interactions. *Phys. Rev. D* **103**, 054025 (2021). <https://doi.org/10.1103/PhysRevD.103.054025>. arXiv:2101.11200
14. K. Azizi, Y. Sarac, H. Sundu, Investigation of hidden-charm double strange pentaquark candidate P_{cs} via its mass and strong decays. *Eur. Phys. J. C* **82**, 543 (2022). <https://doi.org/10.1140/epjc/s10052-022-10495-7>. arXiv:2112.15543
15. J.A. Oller, About meson-baryon scattering with strangeness -1 . in 9th International Conference on Hypernuclear and Strange Particle Physics, 237–242 (2007). https://doi.org/10.1007/978-3-540-76367-3_48
16. D. Cabrera, L. Tolos, J. Aichelin, E. Bratkovskaya, Strange meson-baryon interaction in hot and dense medium: recent progress for a road to GSI/FAIR. *J. Phys.: Conf. Ser.* **668**, 012048 (2016). <https://doi.org/10.1088/1742-6596/668/1/012048>. arXiv:1510.07265
17. A. Feijoo, V.K. Magas, A. Ramos, E. Oset, $\Lambda_b \rightarrow J/\psi K \bar{\Sigma}$ decay and the higher order chiral terms of the meson baryon interaction. *Phys. Rev. D* **92**, 076015 (2015). <https://doi.org/10.1016/j.physletb.2012.05.060>. arXiv:1507.04640. Erratum *ibid.* **D95**, 351 (2017). <https://doi.org/10.1103/PhysRevD.92.076015>
18. L. Roca, M. Mai, E. Oset, U.-G. Meißner, Predictions for the $\Lambda_b \rightarrow J/\psi \Lambda(1405)$ decay. *Eur. Phys. J. C* **75**, 218 (2015). <https://doi.org/10.1140/epjc/s10052-015-3438-1>. arXiv:1503.02936
19. L. Oliver, J.-C. Raynal, R. Sinha, Note on new interesting baryon channels to measure the photon polarization in $b \rightarrow s\gamma$. *Phys. Rev. D* **82**, 117502 (2010). <https://doi.org/10.1103/PhysRevD.82.117502>. arXiv:1007.3632
20. CMS Collaboration, A. Hayrapetyan et al., Observation of the $\Lambda_b^0 \rightarrow J/\psi K^- p$ decay. *Eur. Phys. J. C* **84**, 1062 (2024). <https://doi.org/10.1140/epjc/s10052-024-13114-9>. arXiv:2401.16303
21. M. Pivk, F.R. Le Diberder, sPlot: a statistical tool to unfold data distributions. *Nucl. Instrum. Methods A* **555**, 356 (2005). <https://doi.org/10.1016/j.nima.2005.08.106>. arXiv:physics/0402083
22. H. Dembinski, M. Kenzie, C. Langenbruch, M. Schmelling, Custom orthogonal weight functions (COWs) for event classification. *Nucl. Instrum. Methods A* **1040**, 167270 (2022). <https://doi.org/10.1016/j.nima.2022.167270>. arXiv:2112.04574
23. LHCb Collaboration, A.A. Alves Jr. et al., The LHCb detector at the LHC. *JINST* **3**, S08005 (2008). <https://doi.org/10.1088/1748-0221/3/08/S08005>
24. LHCb Collaboration, R. Aaij et al., LHCb detector performance. *Int. J. Mod. Phys. A* **30**, 1530022 (2015). <https://doi.org/10.1142/S0217751X15300227>. arXiv:1412.6352
25. R. Aaij et al., Design and performance of the LHCb trigger and full real-time reconstruction in Run 2 of the LHC. *JINST* **14**, P04013 (2019). <https://doi.org/10.1088/1748-0221/14/04/P04013>. arXiv:1812.10790
26. T. Sjöstrand, S. Mrenna, P. Skands, PYTHIA 6.4 physics and manual. *JHEP* **05**, 026 (2006). <https://doi.org/10.1088/1126-6708/2006/05/026>. arXiv:hep-ph/0603175
27. I. Belyaev et al., Handling of the generation of primary events in Gauss, the LHCb simulation framework. *J. Phys.: Conf. Ser.* **331**, 032047 (2011). <https://doi.org/10.1088/1742-6596/331/3/032047>
28. D.J. Lange, The EvtGen particle decay simulation package. *Nucl. Instrum. Methods A* **462**, 152 (2001). [https://doi.org/10.1016/S0168-9002\(01\)00089-4](https://doi.org/10.1016/S0168-9002(01)00089-4)
29. N. Davidson, T. Przedzinski, Z. Was, PHOTOS interface in C++: technical and physics documentation. *Comput. Phys. Commun.* **199**, 86 (2016). <https://doi.org/10.1016/j.cpc.2015.09.013>. arXiv:1011.0937
30. Geant4 Collaboration, J. Allison et al., Geant4 developments and applications. *IEEE Trans. Nucl. Sci.* **53**, 270 (2006). <https://doi.org/10.1109/TNS.2006.869826>
31. Geant4 Collaboration, S. Agostinelli et al., Geant4: a simulation toolkit. *Nucl. Instrum. Methods A* **506**, 250 (2003). [https://doi.org/10.1016/S0168-9002\(03\)01368-8](https://doi.org/10.1016/S0168-9002(03)01368-8)
32. M. Clemencic et al., The LHCb simulation application, Gauss: design, evolution and experience. *J. Phys. Conf. Ser.* **331**, 032023 (2011). <https://doi.org/10.1088/1742-6596/331/3/032023>
33. D. Müller, M. Clemencic, G. Corti, M. Gersabeck, ReDecay: a novel approach to speed up the simulation at LHCb. *Eur. Phys. J. C* **78**, 1009 (2018). <https://doi.org/10.1140/epjc/s10052-018-6469-6>. arXiv:1810.10362
34. Particle Data Group, S. Navas et al., Review of particle physics. *Phys. Rev. D* **110**, 030001 (2024). <https://doi.org/10.1103/PhysRevD.110.030001>
35. W.D. Hulsbergen, Decay chain fitting with a Kalman filter. *Nucl. Instrum. Methods A* **552**, 566 (2005). <https://doi.org/10.1016/j.nima.2005.06.078>. arXiv:physics/0503191
36. L. Breiman, J.H. Friedman, R.A. Olshen, C.J. Stone, *Classification and Regression Trees* (Wadsworth International Group, Belmont, 1984)
37. Y. Freund, R.E. Schapire, A decision-theoretic generalization of on-line learning and an application to boosting. *J. Comput. Syst. Sci.* **55**, 119 (1997). <https://doi.org/10.1006/jcss.1997.1504>
38. T. Chen, C. Guestrin, XGBoost: a scalable tree boosting system. <https://doi.org/10.1145/2939672.2939785>. arXiv:1603.02754
39. G. Punzi, Sensitivity of searches for new signals and its optimization. *eConf. C* **030908**, MODT002 (2003). arXiv:physics/0308063
40. R. Aaij et al., Selection and processing of calibration samples to measure the particle identification performance of the LHCb experiment in Run 2. *Eur. Phys. J. Tech. Instrum.* **6**, 1 (2019). <https://doi.org/10.1140/epjti/s40485-019-0050-z>. arXiv:1803.00824
41. LHCb Collaboration, R. Aaij et al., Measurement of the track reconstruction efficiency at LHCb. *JINST* **10**, P02007 (2015). <https://doi.org/10.1088/1748-0221/10/02/P02007>. arXiv:1408.1251
42. D. Martínez Santos, F. Dupertuis, Mass distributions marginalized over per-event errors. *Nucl. Instrum. Methods A* **764**, 150 (2014). <https://doi.org/10.1016/j.nima.2014.06.081>. arXiv:1312.5000
43. T. Skwarnicki, A study of the radiative cascade transitions between the Upsilon-prime and Upsilon resonances. PhD thesis, Institute of Nuclear Physics, Krakow (1986). <http://inspirehep.net/record/230779/>
44. W. Verkerke, D.P. Kirkby, The RooFit toolkit for data modeling. *eConf. C* **0303241**, MOLT007 (2003). arXiv:physics/0306116
45. K. Cranmer, Kernel estimation in high-energy physics. *Comput. Phys. Commun.* **136**, 198 (2001). [https://doi.org/10.1016/S0010-4655\(00\)00243-5](https://doi.org/10.1016/S0010-4655(00)00243-5)
46. N.L. Johnson, Systems of frequency curves generated by methods of translation. *Biometrika* **36**, 149 (1949). <https://doi.org/10.1093/biomet/36.1-2.149>
47. S.S. Wilks, The large-sample distribution of the likelihood ratio for testing composite hypotheses. *Ann. Math. Stat.* **9**, 60 (1938). <https://doi.org/10.1214/aoms/117732360>
48. LHCb Collaboration, L.M. Garcia, L. Henry, B. Kishor, A. Oyanguren, Tracking performance for long-lived particles at LHCb. *J. Phys. Conf. Ser.* **1525**, 012095 (2020). <https://doi.org/10.1088/1742-6596/1525/1/012095>. arXiv:1910.06171
49. LHCb Collaboration, R. Aaij et al., Search for the radiative $\mathcal{E}_b^- \rightarrow \mathcal{E}^- \gamma$ decay. *JHEP* **01**, 069 (2022). [https://doi.org/10.1007/JHEP01\(2022\)069](https://doi.org/10.1007/JHEP01(2022)069). arXiv:2108.07678

LHCb Collaboration*

R. Aaij³⁸, A. S. W. Abdelmotteleb⁵⁷, C. Abellan Beteta⁵¹, F. Abudinén⁵⁷, T. Ackernley⁶¹, A. A. Adefisoye⁶⁹, B. Adeva⁴⁷, M. Adinolfi⁵⁵, P. Adlarson⁸², C. Agapopoulou¹⁴, C. A. Aidala⁸⁴, Z. Ajaltouni¹¹, S. Akar⁶⁶, K. Akiba³⁸, P. Albicocco²⁸, J. Albrecht^{19,f}, F. Alessio⁴⁹, M. Alexander⁶⁰, Z. Aliouche⁶³, P. Alvarez Cartelle⁵⁶, R. Amalric¹⁶, S. Amato³, J. L. Amey⁵⁵, Y. Amhis¹⁴, L. An⁶, L. Anderlini²⁷, M. Andersson⁵¹, A. Andreianov⁴⁴, P. Andreola⁵¹, M. Andreotti²⁶, D. Andreou⁶⁹, A. Anelli^{31.o,49}, D. Ao⁷, F. Archilli^{37.u}, M. Argenton²⁶, S. Arguedas Cuendis^{9,49}, A. Artamonov⁴⁴, M. Artuso⁶⁹, E. Aslanides¹³, R. Ataíde Da Silva⁵⁰, M. Atzeni⁶⁵, B. Audurier¹², D. Bacher⁶⁴, I. Bachiller Perea¹⁰, S. Bachmann²², M. Bachmayer⁵⁰, J. J. Back⁵⁷, P. Baladron Rodriguez⁴⁷, V. Balagura¹⁵, A. Balboni²⁶, W. Baldini²⁶, L. Balzani¹⁹, H. Bao⁷, J. Baptista de Souza Leite⁶¹, C. Barbero Pretel^{12,47}, M. Barbetti²⁷, I. R. Barbosa⁷⁰, R. J. Barlow⁶³, M. Barnyakov²⁵, S. Barsuk¹⁴, W. Barter⁵⁹, J. Bartz⁶⁹, J. M. Basels¹⁷, S. Bashir⁴⁰, G. Bassi^{35.r}, B. Batsukh⁵, P. B. Battista¹⁴, A. Bay⁵⁰, A. Beck⁵⁷, M. Becker¹⁹, F. Bedeschi³⁵, I. B. Bediaga², N. A. Behling¹⁹, S. Belin⁴⁷, K. Belous⁴⁴, I. Belov²⁹, I. Belyaev³⁶, G. Benane¹³, G. Bencivenni²⁸, E. Ben-Haim¹⁶, A. Berezhnoy⁴⁴, R. Bernet⁵¹, S. Bernet Andres⁴⁵, A. Bertolin³³, C. Betancourt⁵¹, F. Betti⁵⁹, J. Bex⁵⁶, I. A. Bezshyiko⁵¹, J. Bhom⁴¹, M. S. Bieker¹⁹, N. V. Biesuz²⁶, P. Billoir¹⁶, A. Biolchini³⁸, M. Birch⁶², F. C. R. Bishop¹⁰, A. Bitadze⁶³, A. Bizzeti, T. Blake⁵⁷, F. Blanc⁵⁰, J. E. Blank¹⁹, S. Blusk⁶⁹, V. Bocharnikov⁴⁴, J. A. Boelhave¹⁹, O. Boente Garcia¹⁵, T. Boettcher⁶⁶, A. Bohare⁵⁹, A. Boldyrev⁴⁴, C. S. Bolognani⁷⁹, R. Bolzonella^{26.1}, R. B. Bonacci¹, N. Bondar⁴⁴, A. Bordellius⁴⁹, F. Borgato³³, S. Borghi⁶³, M. Borsato^{31.o}, J. T. Borsuk⁴¹, E. Bottalico⁶¹, S. A. Bouchiba⁵⁰, M. Bovill⁶⁴, T. J. V. Bowcock⁶¹, A. Boyer⁴⁹, C. Bozzi²⁶, J. D. Brandenburg⁸⁵, A. Brea Rodriguez⁵⁰, N. Breer¹⁹, J. Brodzicka⁴¹, A. Brossa Gonzalo^{47.*}, J. Brown⁶¹, D. Brundu³², E. Buchanan⁵⁹, L. Buonincontri^{33.p}, M. Burgos Marcos⁷⁹, A. T. Burke⁶³, C. Burr⁴⁹, J. S. Butter⁵⁶, J. Buytaert⁴⁹, W. Byczynski⁴⁹, S. Cadettu³², H. Cai⁷⁴, A. C. Caillet¹⁶, R. Calabrese^{26.1}, S. Calderon Ramirez⁹, L. Calefice⁴⁶, S. Cali²⁸, M. Calvi^{31.o}, M. Calvo Gomez⁴⁵, P. Camargo Magalhaes^{2.z}, J. I. Cambon Bouzas⁴⁷, P. Campana²⁸, D. H. Campora Perez⁷⁹, A. F. Campoverde Quezada⁷, S. Capelli³¹, L. Capriotti²⁶, R. Caravaca-Mora⁹, A. Carbone^{25.j}, L. Carcedo Salgado⁴⁷, R. Cardinale^{29.m}, A. Cardini³², P. Carniti^{31.o}, L. Carus²², A. Casais Vidal⁶⁵, R. Caspary²², G. Casse⁶¹, M. Cattaneo⁴⁹, G. Cavallero^{26,49}, V. Cavallini^{26.1}, S. Celani²², S. Cesare^{30.n}, A. J. Chadwick⁶¹, I. Chahrour⁸⁴, M. Charles¹⁶, Ph. Charpentier⁴⁹, E. Chatzianagnostou³⁸, M. Chefdeville¹⁰, C. Chen¹³, S. Chen⁵, Z. Chen⁷, A. Chernov⁴¹, S. Chernyshenko⁵³, X. Chiotopoulos⁷⁹, V. Chobanova⁸¹, M. Chruszcz⁴¹, A. Chubykin⁴⁴, V. Chulikov^{28,36}, P. Ciambone²⁸, X. Cid Vidal⁴⁷, G. Ciezarek⁴⁹, P. Cifra⁴⁹, P. E. L. Clarke⁵⁹, M. Clemencic⁴⁹, H. V. Cliff⁵⁶, J. Closier⁴⁹, C. Cocha Toapaxi²², V. Coco⁴⁹, J. Cogan¹³, E. Cogneras¹¹, L. Cojocariu⁴³, S. Collaviti⁵⁰, P. Collins⁴⁹, T. Colombo⁴⁹, M. C. Colonna¹⁹, A. Comerma-Montells⁴⁶, L. Congedo²⁴, A. Contu³², N. Cooke⁶⁰, I. Corredoira⁴⁷, A. Correia¹⁶, G. Corti⁴⁹, J. J. Cottee Meldrum⁵⁵, B. Couturier⁴⁹, D. C. Craik⁵¹, M. Cruz Torres^{2.g}, E. Curras Rivera⁵⁰, R. Currie⁵⁹, C. L. Da Silva⁶⁸, S. Dadabaev⁴⁴, L. Dai⁷¹, X. Dai⁶, E. Dall'Occo⁴⁹, J. Dalseno⁴⁷, C. D'Ambrosio⁴⁹, J. Daniel¹¹, A. Danilina⁴⁴, P. d'Argent²⁴, G. Darze³, A. Davidson⁵⁷, J. E. Davies⁶³, O. De Aguiar Francisco⁶³, C. De Angelis^{32.k}, F. De Benedetti⁴⁹, J. de Boer³⁸, K. De Bruyn⁷⁸, S. De Capua⁶³, M. De Cian²², U. De Freitas Carneiro Da Graca^{2.a}, E. De Lucia²⁸, J. M. De Miranda², L. De Paula³, M. De Serio^{24.h}, P. De Simone²⁸, F. De Vellis¹⁹, J. A. de Vries⁷⁹, F. Debernardis²⁴, D. Decamp¹⁰, V. Dedu¹³, S. Dekkers¹, L. Del Buono¹⁶, B. Delaney⁶⁵, H.-P. Dembinski¹⁹, J. Deng⁸, V. Denysenko⁵¹, O. Deschamps¹¹, F. Dettori^{32.k}, B. Dey⁷⁷, P. Di Nezza²⁸, I. Diachkov⁴⁴, S. Didenko⁴⁴, S. Ding⁶⁹, L. Dittmann²², V. Dobishuk⁵³, A. D. Docheva⁶⁰, C. Dong^{4.b}, A. M. Donohoe²³, F. Dordei³², A. C. dos Reis², A. D. Dowling⁶⁹, W. Duan⁷², P. Duda⁸⁰, M. W. Dudek⁴¹, L. Dufour⁴⁹, V. Duk³⁴, P. Durante⁴⁹, M. M. Duras⁸⁰, J. M. Durham⁶⁸, O. D. Durmus⁷⁷, A. Dziurda⁴¹, A. Dzyuba⁴⁴, S. Easo⁵⁸, E. Eckstein¹⁸, U. Egede¹, A. Egorychev⁴⁴, V. Egorychev⁴⁴, S. Eisenhardt⁵⁹, E. Ejopu⁶³, L. Eklund⁸², M. Elashri⁶⁶, J. Ellbracht¹⁹, S. Ely⁶², A. Ene⁴³, J. Eschle⁶⁹, S. Esen²², T. Evans⁶³, F. Fabiano³², L. N. Falcao², Y. Fan⁷, B. Fang⁷, L. Fantini^{34.q,49}, M. Faria⁵⁰, K. Farmer⁵⁹, D. Fazzini^{31.o}, L. Felkowski⁸⁰, M. Feng^{5.7}, M. Feo², A. Fernandez Casani⁴⁸, M. Fernandez Gomez⁴⁷, A. D. Fernez⁶⁷, F. Ferrari²⁵, F. Ferreira Rodrigues³, M. Ferrillo⁵¹, M. Ferro-Luzzi⁴⁹, S. Filippov⁴⁴, R. A. Fini²⁴, M. Fiorini^{26.1}, M. Firlej⁴⁰, K. L. Fischer⁶⁴, D. S. Fitzgerald⁸⁴, C. Fitzpatrick⁶³, T. Fiutowski⁴⁰, F. Fleuret¹⁵, M. Fontana²⁵, L. F. Foreman⁶³, R. Forty⁴⁹, D. Foulds-Holt⁵⁶, V. Franco Lima³, M. Franco Sevilla⁶⁷, M. Frank⁴⁹, E. Franzoso^{26.1}, G. Frau⁶³, C. Frei⁴⁹, D. A. Friday⁶³, J. Fu⁷, Q. Fühning^{19.f,56}

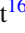












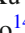



















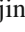
















Y. Fujii¹, T. Fulghesu¹⁶, E. Gabriel³⁸, G. Galati²⁴, M. D. Galati³⁸, A. Gallas Torreira⁴⁷, D. Galli^{25,j}, S. Gambetta⁵⁹, M. Gandelman³, P. Gandini³⁰, B. Ganie⁶³, H. Gao⁷, R. Gao⁶⁴, T. Q. Gao⁵⁶, Y. Gao⁸, Y. Gao⁶, Y. Gao⁸, L. M. Garcia Martin⁵⁰, P. Garcia Moreno⁴⁶, J. García Pardiñas⁴⁹, P. Gardner⁶⁷, K. G. Garg⁸, L. Garrido⁴⁶, C. Gaspar⁴⁹, L. L. Gerken¹⁹, E. Gersabeck⁶³, M. Gersabeck²⁰, T. Gershon⁵⁷, S. G. Ghizzo^{29,m}, Z. Ghorbanimoghaddam⁵⁵, L. Giambastiani^{33,p}, F. I. Giasemis^{16,e}, V. Gibson⁵⁶, H. K. Giemza⁴², A. L. Gilman⁶⁴, M. Giovannetti²⁸, A. Gioventù⁴⁶, L. Girardey⁶³, C. Giugliano^{26,1}, M. A. Giza⁴¹, E. L. Gkoukousis⁶², F. C. Glaser^{14,22}, V. V. Gligorov^{16,49}, C. Göbel⁷⁰, L. Golinka-Bezshyyko⁸³, E. Golobardes⁴⁵, D. Golubkov⁴⁴, A. Golutvin^{44,49,62}, S. Gomez Fernandez⁴⁶, W. Gomulka⁴⁰, F. Goncalves Abrantes⁶⁴, M. Goncerz⁴¹, G. Gong^{4,b}, J. A. Gooding¹⁹, I. V. Gorelov⁴⁴, C. Gotti³¹, E. Govorkova⁶⁵, J. P. Grabowski¹⁸, L. A. Granado Cardoso⁴⁹, E. Graugés⁴⁶, E. Graverini^{50,s}, L. Grazette⁵⁷, G. Graziani, A. T. Grecu⁴³, L. M. Greeven³⁸, N. A. Grieser⁶⁶, L. Grillo⁶⁰, S. Gromov⁴⁴, C. Gu¹⁵, M. Guarise²⁶, L. Guerry¹¹, V. Guliaeva⁴⁴, P. A. Günther²², A.-K. Guseinov⁵⁰, E. Gushchin⁴⁴, Y. Guz^{6,44,49}, T. Gys⁴⁹, K. Habermann¹⁸, T. Hadavizadeh¹, C. Hadjivasiliou⁶⁷, G. Haefeli⁵⁰, C. Haen⁴⁹, G. Hallett⁵⁷, M. M. Halvorsen⁴⁹, P. M. Hamilton⁶⁷, J. Hammerich⁶¹, Q. Han³³, X. Han^{22,49}, S. Hansmann-Menzemer²², L. Hao⁷, N. Harnew⁶⁴, T. H. Harris¹, M. Hartmann¹⁴, S. Hashmi⁴⁰, J. He^{7,c}, F. Hemmer⁴⁹, C. Henderson⁶⁶, R. D. L. Henderson^{1,57}, A. M. Hennequin⁴⁹, K. Hennessy⁶¹, L. Henry⁵⁰, J. Herd⁶², P. Herrero Gascon²², J. Heuel¹⁷, A. Hicheur³, G. Hijano Mendizabal⁵¹, J. Horswill⁶³, R. Hou⁸, Y. Hou¹¹, N. Howarth⁶¹, J. Hu⁷², W. Hu⁶, X. Hu^{4,b}, W. Huang⁷, W. Hulsbergen³⁸, R. J. Hunter⁵⁷, M. Hushchyn⁴⁴, D. Hutchcroft⁶¹, M. Idzik⁴⁰, D. Ilin⁴⁴, P. Ilten⁶⁶, A. Inglessi⁴⁴, A. Iniukhin⁴⁴, A. Ishteev⁴⁴, K. Ivshin⁴⁴, R. Jacobsson⁴⁹, H. Jage¹⁷, S. J. Jaimes Elles^{49,48,75}, S. Jakobsen⁴⁹, E. Jans³⁸, B. K. Jashal⁴⁸, A. Jawahery⁶⁷, V. Jevtic^{19,f}, E. Jiang⁶⁷, X. Jiang^{5,7}, Y. Jiang⁷, Y. J. Jiang⁶, M. John⁶⁴, A. John Rubesh Rajan²³, D. Johnson⁵⁴, C. R. Jones⁵⁶, T. P. Jones⁵⁷, S. Joshi⁴², B. Jost⁴⁹, J. Juan Castella⁵⁶, N. Jurik⁴⁹, I. Juszczak⁴¹, D. Kaminaris⁵⁰, S. Kandybei⁵², M. Kane⁵⁹, Y. Kang^{4,b}, C. Kar¹¹, M. Karacson⁴⁹, D. Karpenkov⁴⁴, A. Kauniskangas⁵⁰, J. W. Kautz⁶⁶, M. K. Kazanecki⁴¹, F. Keizer⁴⁹, M. Kenzie⁵⁶, T. Ketel³⁸, B. Khanji⁶⁹, A. Kharisova⁴⁴, S. Kholodenko^{35,49}, G. Khreich¹⁴, T. Kim¹⁷, V. S. Kirsebom³¹, O. Kitouni⁶⁵, S. Klaver³⁹, N. Kleijne^{35,r}, K. Klimaszewski⁴², M. R. Kmiec⁴², S. Koliiev⁵³, L. Kolk¹⁹, A. Konoplyannikov⁴⁴, P. Kopciwicz⁴⁹, P. Koppenburg³⁸, M. Korolev⁴⁴, I. Kostiuik³⁸, O. Kot⁵³, S. Kotriakhova, A. Kozachuk⁴⁴, P. Kravchenko⁴⁴, L. Kravchuk⁴⁴, M. Kreps⁵⁷, P. Krokovny⁴⁴, W. Krupa⁶⁹, W. Krzemien⁴², O. Kshyvanskyi⁵³, S. Kubis⁸⁰, M. Kucharczyk⁴¹, V. Kudryavtsev⁴⁴, E. Kulikova⁴⁴, A. Kupsc⁸², B. K. Kutsenko¹³, D. Lacarrere⁴⁹, P. Laguarda Gonzalez⁴⁶, A. Lai³², A. Lampis³², D. Lancierini⁵⁶, C. Landesa Gomez⁴⁷, J. J. Lane¹, R. Lane⁵⁵, G. Lanfranchi²⁸, C. Langenbruch²², J. Langer¹⁹, O. Lantwin⁴⁴, T. Latham⁵⁷, F. Lazzari^{35,s,49}, C. Lazzeroni⁵⁴, R. Le Gac¹³, H. Lee⁶¹, R. Lefèvre¹¹, A. Leflat⁴⁴, S. Legotin⁴⁴, M. Lehurax⁵⁷, E. Lemos Cid⁴⁹, O. Leroy¹³, T. Lesiak⁴¹, E. D. Lesser⁴⁹, B. Leverington²², A. Li^{4,b}, C. Li¹³, H. Li⁷², K. Li⁸, L. Li⁶³, M. Li⁸, P. Li⁷, P.-R. Li⁷³, Q. Li^{5,7}, S. Li⁸, T. Li^{5,d}, T. Li⁷², Y. Li⁸, Y. Li⁵, Z. Lian^{4,b}, X. Liang⁶⁹, S. Libralon⁴⁸, C. Lin⁷, T. Lin⁵⁸, R. Lindner⁴⁹, H. Linton⁶², V. Lisovskyi⁵⁰, R. Litvinov^{32,49}, F. L. Liu¹, G. Liu⁷², K. Liu⁷³, S. Liu^{5,7}, W. Liu⁸, Y. Liu⁵⁹, Y. Liu⁷³, Y. L. Liu⁶², G. Loachamin Ordonez⁷⁰, A. Lobo Salvia⁴⁶, A. Loi³², T. Long⁵⁶, J. H. Lopes³, A. Lopez Huertas⁴⁶, S. L.ópez Soliño⁴⁷, Q. Lu¹⁵, C. Lucarelli²⁷, D. Lucchesi^{33,p}, M. Lucio Martinez⁷⁹, V. Lukashenko^{38,53}, Y. Luo⁶, A. Lupato^{33,i}, E. Luppi^{26,1}, K. Lynch²³, X.-R. Lyu⁷, G. M. Ma^{4,b}, S. Maccolini¹⁹, F. Machefer¹⁴, F. Maciuc⁴³, B. Mack⁶⁹, I. Mackay⁶⁴, L. M. Mackey⁶⁹, L. R. Madhan Mohan⁵⁶, M. J. Madurai⁵⁴, A. Maevskiy⁴⁴, D. Magdalinski³⁸, D. Maisuzenko⁴⁴, J. J. Malczewski⁴¹, S. Malde⁶⁴, L. Malentacca⁴⁹, A. Malinin⁴⁴, T. Maltsev⁴⁴, G. Manca^{32,k}, G. Mancinelli¹³, C. Mancuso³⁰, R. Manera Escalero⁴⁶, F. M. Manganello³⁷, D. Manuzzi²⁵, D. Marangotto^{30,n}, J. F. Marchand¹⁰, R. Marchevski⁵⁰, U. Marconi²⁵, E. Mariani¹⁶, S. Mariani⁴⁹, C. Marin Benito⁴⁶, J. Marks²², A. M. Marshall⁵⁵, L. Martel⁶⁴, G. Martelli^{34,q}, G. Martellotti³⁶, L. Martinazzoli⁴⁹, M. Martinelli^{31,o}, D. Martinez Gomez⁷⁸, D. Martinez Santos⁸¹, F. Martinez Vidal⁴⁸, A. Martorell i Granollers⁴⁵, A. Massafferri², R. Matev⁴⁹, A. Mathad⁴⁹, V. Matiunin⁴⁴, C. Matteuzzi⁶⁹, K. R. Mattioli¹⁵, A. Mauri⁶², E. Maurice¹⁵, J. Mauricio⁴⁶, P. Mayencourt⁵⁰, J. Mazorra de Cos⁴⁸, M. Mazurek⁴², M. McCann⁶², T. H. McGrath⁶³, N. T. McHugh⁶⁰, A. McNab⁶³, R. McNulty²³, B. Meadows⁶⁶, G. Meier¹⁹, D. Melnychuk⁴², F. M. Meng^{4,b}, M. Merk^{38,79}, A. Merli⁵⁰, L. Meyer Garcia⁶⁷, D. Miao^{5,7}, H. Miao⁷, M. Mikhasenko⁷⁶, D. A. Milanes^{75,x}, A. Minotti^{31,o}, E. Minucci²⁸, T. Miralles¹¹, B. Mitreska¹⁹, D. S. Mittel¹⁹, A. Modak⁵⁸, L. Moeser¹⁹, R. A. Mohammed⁶⁴, R. D. Moise¹⁷, S. Mokhnenko⁴⁴, E. F. Molina Cardenas⁸⁴, T. Mombächer⁴⁹, M. Monk^{57,1}, S. Monteil¹¹,

A. Morcillo Gomez⁴⁷ , G. Morello²⁸ , M. J. Morello^{35,r} , M. P. Morgenthaler²² , J. Moron⁴⁰ , W. Morren³⁸ , A. B. Morris⁴⁹ , A. G. Morris¹³ , R. Mountain⁶⁹ , H. Mu^{4,b} , Z. M. Mu⁶ , E. Muhammad⁵⁷ , F. Muheim⁵⁹ , M. Mulder⁷⁸ , K. Müller⁵¹ , F. Muñoz-Rojas⁹ , R. Murta⁶² , P. Naik⁶¹ , T. Nakada⁵⁰ , R. Nandakumar⁵⁸ , T. Nanut⁴⁹ , I. Nasteva³ , M. Needham⁵⁹ , N. Neri^{30,n} , S. Neubert¹⁸ , N. Neufeld⁴⁹ , P. Neustroev⁴⁴ , J. Nicolini¹⁹ , D. Nicotra⁷⁹ , E. M. Niel⁴⁹ , N. Nikitin⁴⁴ , P. Nogarolli³ , P. Nogga¹⁸ , C. Normand⁵⁵ , J. Novoa Fernandez⁴⁷ , G. Nowak⁶⁶ , C. Nunez⁸⁴ , H. N. Nur⁶⁰ , A. Oblakowska-Mucha⁴⁰ , V. Obraztsov⁴⁴ , T. Oeser¹⁷ , S. Okamura^{26,1} , A. Okhotnikov⁴⁴ , O. Okhrimenko⁵³ , R. Oldeman^{32,k} , F. Oliva⁵⁹ , M. Olocco¹⁹ , C. J. G. Onderwater⁷⁹ , R. H. O'Neil⁴⁹ , D. Osthues¹⁹ , J. M. Otalora Goicochea³ , P. Owen⁵¹ , A. Oyanguren⁴⁸

, O. Ozcelik⁵⁹ , F. Paciolla^{35,v} , A. Padee⁴² , K. O. Padeken¹⁸ , B. Pagare⁵⁷ , P. R. Pais²² , T. Pajero⁴⁹ , A. Palano²⁴ , M. Palutan²⁸ , X. Pan^{4,b} , G. Panshin⁴⁴ , L. Paolucci⁵⁷ , A. Papanestis^{58,49} , M. Pappagallo^{24,h} , L. L. Pappalardo^{26,1} , C. Pappenheimer⁶⁶ , C. Parkes⁶³ , D. Parmar⁷⁶ , B. Passalacqua^{26,1} , G. Passaleva²⁷ , D. Passaro^{35,r,49} , A. Pastore²⁴ , M. Patel⁶² , J. Patoc⁶⁴ , C. Patrignani^{25,j} , A. Paul⁶⁹ , C. J. Pawley⁷⁹ , A. Pellegrino³⁸ , J. Peng^{5,7} , M. Pepe Altarelli²⁸ , S. Perazzini²⁵ , D. Pereima⁴⁴ , H. Pereira Da Costa⁶⁸ , A. Pereiro Castro⁴⁷ , P. Perret¹¹ , A. Perrevoort⁷⁸ , A. Perro⁴⁹ , M. J. Peters⁶⁶ , K. Petridis⁵⁵ , A. Petrolini^{29,m} , J. P. Pfaller⁶⁶ , H. Pham⁶⁹ , L. Pica^{35,r} , M. Piccini³⁴ , L. Piccolo³² , B. Pietrzyk¹⁰ , G. Pietrzyk¹⁴ , R. N. Pilato⁶¹ , D. Pinci³⁶ , F. Pisani⁴⁹ , M. Pizzichemi^{31,o,49} , V. Placinta⁴³ , M.
Plo Casasus⁴⁷ , T. Poeschl⁴⁹ , F. Polci¹⁶ , M. Poli Lener²⁸ , A. Poluektov¹³ , N. Polukhina⁴⁴ , I. Polyakov⁴⁴ , E. Polycarpo³ , S. Ponce⁴⁹ , D. Popov⁷ , S. Poslavskii⁴⁴ , K. Prasanth⁵⁹ , C. Prouve⁸¹ , D. Provenzano^{32,k} , V. Pugatch⁵³ , G. Punzi^{35,s} , S. Qasim⁵¹ , Q. Q. Qian⁶ , W. Qian⁷ , N. Qin^{4,b} , S. Qu^{4,b} , R. Quagliani⁴⁹ , R. I. Rabadan Trejo⁵⁷ , J. H. Rademacker⁵⁵ , M. Rama³⁵ , M. Ramírez García⁸⁴ , V. Ramos De Oliveira⁷⁰ , M. Ramos Pernas⁵⁷ , M. S. Rangel³ , F. Ratnikov⁴⁴ , G. Raven³⁹ , M. Rebollo De Miguel⁴⁸ , F. Redi^{30,i} , J. Reich⁵⁵ , F. Reiss²⁰ , Z. Ren⁷ , P. K. Resmi⁶⁴ , M. Ribalda Galvez⁴⁶ , R. Ribatti⁵⁰ , G. R. Ricart^{12,15} , D. Riccardi^{35,r} , S. Ricciardi⁵⁸ , K. Richardson⁶⁵ , M. Richardson-Slipper⁵⁹ , K. Rinnert⁶¹ , P. Robbe^{14,49} , G. Robertson⁶⁰ , E. Rodrigues⁶¹ , A. Rodriguez Alvarez⁴⁶ , E. Rodriguez Fernandez⁴⁷ , J. A. Rodriguez Lopez⁷⁵ , E. Rodriguez Rodriguez⁴⁹

, J. Roensch¹⁹ , A. Rogachev⁴⁴ , A. Rogovskiy⁵⁸ , D. L. Rolf⁴⁹ , P. Roloff⁴⁹ , V. Romanovskiy⁶⁶ , A. Romero Vidal⁴⁷ , G. Romolini²⁶ , F. Ronchetti⁵⁰ , T. Rong⁶ , M. Rotondo²⁸ , S. R. Roy²² , M. S. Rudolph⁶⁹ , M. Ruiz Diaz²² , R. A. Ruiz Fernandez⁴⁷ , J. Ruiz Vidal^{82,aa} , J. Ryzka⁴⁰ , J. J. Saavedra-Arias⁹ , J. J. Saborido Silva⁴⁷ , R. Sadek¹⁵ , N. Sagidova⁴⁴ , D. Sahoo⁷⁷ , N. Sahoo⁵⁴ , B. Saitta^{32,k} , M. Salomoni^{31,49,o} , I. Sanderswood⁴⁸ , R. Santacesaria³⁶ , C. Santamarina Rios⁴⁷ , M. Santimaria²⁸ , L. Santoro² , E. Santovetti³⁷ , A. Saputi^{26,49} , D. Saranin⁴⁴ , A. Sarnatskiy⁷⁸ , G. Sarpis⁵⁹ , M. Sarpis⁶³ , C. Satriano^{36,t} , A. Satta³⁷ , M. Saur⁶ , D. Savrina⁴⁴ , H. Sazak¹⁷ , F. Sborzacchi^{28,49} , L. G. Scantlebury Smead⁶⁴ , A. Scarabotto¹⁹ , S. Schael¹⁷ , S. Scherl⁶¹ , M. Schiller⁶⁰ , H. Schindler⁴⁹ , M. Schmelling²¹ , B. Schmidt⁴⁹ , S. Schmitt¹⁷ , H. Schmitz¹⁸ , O.
Schneider⁵⁰ , A. Schopper⁴⁹ , N. Schulte¹⁹ , S. Schulte⁵⁰ , M. H. Schune¹⁴ , R. Schwemmer⁴⁹ , G. Schwering¹⁷ , B. Sciascia²⁸ , A. Sciuccati⁴⁹ , I. Segal⁷⁶ , S. Sellam⁴⁷ , A. Semennikov⁴⁴ , T. Senger⁵¹ , M. Senghi Soares³⁹ , A. Sergi^{29,m} , N. Serra⁵¹ , L. Sestini³³ , A. Seuthe¹⁹ , Y. Shang⁶ , D. M. Shangase⁸⁴ , M. Shapkin⁴⁴ , R. S. Sharma⁶⁹ , I. Shchemerov⁴⁴ , L. Shchutska⁵⁰ , T. Shears⁶¹ , L. Shekhtman⁴⁴ , Z. Shen⁶ , S. Sheng^{5,7} , V. Shevchenko⁴⁴ , B. Shi⁷ , Q. Shi⁷ , Y. Shimizu¹⁴ , E. Shmanin²⁵ , R. Shorkin⁴⁴ , J. D. Shupperd⁶⁹ , R. Silva Coutinho⁶⁹ , G. Simi^{33,p} , S. Simone^{24,h} , N. Skidmore⁵⁷ , T. Skwarnicki⁶⁹ , M. W. Slater⁵⁴ , J. C. Smallwood⁶⁴ , E. Smith⁶⁵ , K. Smith⁶⁸ , M. Smith⁶² , A. Snoch³⁸ , L. Soares Lavra⁵⁹ , M. D. Sokoloff⁶⁶ , F. J. P. Soler⁶⁰ , A. Solomin^{44,55} , A. Solovov⁴⁴ , I. Solovvey⁴⁴ , N. S. Sommerfeld¹⁸

, R. Song¹ , Y. Song⁵⁰ , Y. Song^{4,b} , Y. S. Song⁶ , F. L. Souza De Almeida⁶⁹ , B. Souza De Paula³ , E. Spadaro Norella^{29,m} , E. Spedicato²⁵ , J. G. Speer¹⁹ , E. Spiridenkov⁴⁴ , P. Spradlin⁶⁰ , V. Sriskaran⁴⁹ , F. Stagni⁴⁹ , M. Stahl⁷⁶ , S. Stahl⁴⁹ , S. Stanislaus⁶⁴ , M. Stefaniak⁸⁵ , E. N. Stein⁴⁹ , O. Steinkamp⁵¹ , O. Stenyakin⁴⁴ , H. Stevens¹⁹ , D. Strelalina⁴⁴ , Y. Su⁷ , F. Suljik⁶⁴ , J. Sun³² , L. Sun⁷⁴ , D. Sundfeld² , W. Sutcliffe⁵¹ , P. N. Swallow⁵⁴ , K. Swientek

M. Vieites Diaz⁴⁷ , X. Vilasis-Cardona⁴⁵ , E. Vilella Figueras⁶¹ , A. Villa²⁵ , P. Vincent¹⁶ , F. C. Volle⁵⁴ , D. vom Bruch¹³ , N. Voropaev⁴⁴ , K. Vos⁷⁹ , C. Vrahas⁵⁹ , J. Wagner¹⁹ , J. Walsh³⁵ , E. J. Walton^{1,57} , G. Wan⁶ , C. Wang²² , G. Wang⁸ , J. Wang⁶ , J. Wang⁵ , J. Wang^{4,b} , J. Wang⁷⁴ , M. Wang⁴⁹ , N. W. Wang⁷ , R. Wang⁵⁵ , X. Wang⁸ , X. Wang⁷² , X. W. Wang⁶² , Y. Wang⁶ , Z. Wang¹⁴ , Z. Wang^{4,b} , Z. Wang³⁰ , J. A. Ward^{57,1} , M. Waterlaet⁴⁹ , N. K. Watson⁵⁴ , D. Websdale⁶² , Y. Wei⁶ , J. Wendel⁸¹ , B. D. C. Westhenry⁵⁵ , C. White⁵⁶ , M. Whitehead⁶⁰ , E. Whiter⁵⁴ , A. R. Wiederhold⁶³ , D. Wiedner¹⁹ , G. Wilkinson⁶⁴ , M. K. Wilkinson⁶⁶ , M. Williams⁶⁵ , M. J. Williams⁴⁹ , M. R. J. Williams⁵⁹ , R. Williams⁵⁶ , Z. Williams⁵⁵ , F. F. Wilson⁵⁸ , M. Winn¹² , W. Wislicki⁴² , M. Witek⁴¹ , L. Witola²² , G. Wormser¹⁴ , S. A. Wotton⁵⁶ , H. Wu⁶⁹ , J. Wu⁸ , X. Wu⁷⁴ , Y. Wu⁶ , Z. Wu⁷ , K. Wyllie⁴⁹ , S. Xian⁷² , Z. Xiang⁵ , Y. Xie⁸ , T. X. Xing³⁰ , A. Xu³⁵ , L. Xu^{4,b} , L. Xu^{4,b} , M. Xu⁵⁷ , Z. Xu⁴⁹ , Z. Xu⁷ , Z. Xu⁵ , K. Yang⁶² , S. Yang⁷ , X. Yang⁶ , Y. Yang^{29,m} , Z. Yang⁶ , V. Yeroshenko¹⁴ , H. Yeung⁶³ , H. Yin⁸ , X. Yin⁷ , C. Y. Yu⁶ , J. Yu⁷¹ , X. Yuan⁵ , Y. Yuan^{5,7} , E. Zaffaroni⁵⁰ , M. Zavertyaev²¹ , M. Zdybal⁴¹ , F. Zenesini²⁵ , C. Zeng^{5,7} , M. Zeng^{4,b} , C. Zhang⁶ , D. Zhang⁸ , J. Zhang⁷ , L. Zhang^{4,b} , S. Zhang⁷¹ , S. Zhang⁶⁴ , Y. Zhang⁶ , Y. Z. Zhang^{4,b} , Z. Zhang^{4,b} , Y. Zhao²² , A. Zhelezov²² , S. Z. Zheng⁶ , X. Z. Zheng^{4,b} , Y. Zheng⁷ , T. Zhou⁶ , X. Zhou⁸ , Y. Zhou⁷ , V. Zhovkovska⁵⁷ , L. Z. Zhu⁷ , X. Zhu^{4,b} , X. Zhu⁸ , V. Zhukov¹⁷ , J. Zhuo⁴⁸ , Q. Zou^{5,7} , D. Zuliani^{33,p} , G. Zunica⁵⁰ 

¹ School of Physics and Astronomy, Monash University, Melbourne, Australia

² Centro Brasileiro de Pesquisas Físicas (CBPF), Rio de Janeiro, Brazil

³ Universidade Federal do Rio de Janeiro (UFRJ), Rio de Janeiro, Brazil

⁴ Department of Engineering Physics, Tsinghua University, Beijing, China

⁵ Institute of High Energy Physics (IHEP), Beijing, China

⁶ School of Physics State Key Laboratory of Nuclear Physics and Technology, Peking University, Beijing, China

⁷ University of Chinese Academy of Sciences, Beijing, China

⁸ Institute of Particle Physics, Central China Normal University, Wuhan, Hubei, China

⁹ Consejo Nacional de Rectores (CONARE), San Jose, Costa Rica

¹⁰ Université Savoie Mont Blanc, CNRS, IN2P3-LAPP, Annecy, France

¹¹ Université Clermont Auvergne, CNRS/IN2P3, LPC, Clermont-Ferrand, France

¹² Université Paris-Saclay, Centre d'Etudes de Saclay (CEA), IRFU, Saclay, Gif-sur-Yvette, France

¹³ Aix Marseille Univ, CNRS/IN2P3, CPPM, Marseille, France

¹⁴ Université Paris-Saclay, CNRS/IN2P3, IJCLab, Orsay, France

¹⁵ Laboratoire Leprince-Ringuet, CNRS/IN2P3, Ecole Polytechnique, Institut Polytechnique de Paris, Palaiseau, France

¹⁶ LPNHE, Sorbonne Université, Paris Diderot Sorbonne Paris Cité, CNRS/IN2P3, Paris, France

¹⁷ I. Physikalisches Institut, RWTH Aachen University, Aachen, Germany

¹⁸ Universität Bonn-Helmholtz-Institut für Strahlen und Kernphysik, Bonn, Germany

¹⁹ Fakultät Physik, Technische Universität Dortmund, Dortmund, Germany

²⁰ Physikalisches Institut, Albert-Ludwigs-Universität Freiburg, Freiburg, Germany

²¹ Max-Planck-Institut für Kernphysik (MPIK), Heidelberg, Germany

²² Physikalisches Institut, Ruprecht-Karls-Universität Heidelberg, Heidelberg, Germany

²³ School of Physics, University College Dublin, Dublin, Ireland

²⁴ INFN Sezione di Bari, Bari, Italy

²⁵ INFN Sezione di Bologna, Bologna, Italy

²⁶ INFN Sezione di Ferrara, Ferrara, Italy

²⁷ INFN Sezione di Firenze, Firenze, Italy

²⁸ INFN Laboratori Nazionali di Frascati, Frascati, Italy

²⁹ INFN Sezione di Genova, Genoa, Italy

³⁰ INFN Sezione di Milano, Milan, Italy

³¹ INFN Sezione di Milano-Bicocca, Milan, Italy

³² INFN Sezione di Cagliari, Monserrato, Italy

³³ INFN Sezione di Padova, Padua, Italy

³⁴ INFN Sezione di Perugia, Perugia, Italy

³⁵ INFN Sezione di Pisa, Pisa, Italy

³⁶ INFN Sezione di Roma La Sapienza, Rome, Italy

- ³⁷ INFN Sezione di Roma Tor Vergata, Rome, Italy
- ³⁸ Nikhef National Institute for Subatomic Physics, Amsterdam, The Netherlands
- ³⁹ Nikhef National Institute for Subatomic Physics and VU University Amsterdam, Amsterdam, The Netherlands
- ⁴⁰ AGH-University of Krakow, Faculty of Physics and Applied Computer Science, Kraków, Poland
- ⁴¹ Henryk Niewodniczanski Institute of Nuclear Physics Polish Academy of Sciences, Kraków, Poland
- ⁴² National Center for Nuclear Research (NCBJ), Warsaw, Poland
- ⁴³ Horia Hulubei National Institute of Physics and Nuclear Engineering, Bucharest-Magurele, Romania
- ⁴⁴ Affiliated with an Institute Covered by a Cooperation Agreement with CERN, Geneva, Switzerland
- ⁴⁵ DS4DS, La Salle, Universitat Ramon Llull, Barcelona, Spain
- ⁴⁶ ICCUB, Universitat de Barcelona, Barcelona, Spain
- ⁴⁷ Instituto Galego de Física de Altas Enerxías (IGFAE), Universidade de Santiago de Compostela, Santiago de Compostela, Spain
- ⁴⁸ Instituto de Física Corpuscular, Centro Mixto Universidad de Valencia-CSIC, Valencia, Spain
- ⁴⁹ European Organization for Nuclear Research (CERN), Geneva, Switzerland
- ⁵⁰ Institute of Physics, Ecole Polytechnique Fédérale de Lausanne (EPFL), Lausanne, Switzerland
- ⁵¹ Physik-Institut, Universität Zürich, Zurich, Switzerland
- ⁵² NSC Kharkiv Institute of Physics and Technology (NSC KIPT), Kharkiv, Ukraine
- ⁵³ Institute for Nuclear Research of the National Academy of Sciences (KINR), Kyiv, Ukraine
- ⁵⁴ School of Physics and Astronomy, University of Birmingham, Birmingham, UK
- ⁵⁵ H.H. Wills Physics Laboratory, University of Bristol, Bristol, UK
- ⁵⁶ Cavendish Laboratory, University of Cambridge, Cambridge, UK
- ⁵⁷ Department of Physics, University of Warwick, Coventry, UK
- ⁵⁸ STFC Rutherford Appleton Laboratory, Didcot, UK
- ⁵⁹ School of Physics and Astronomy, University of Edinburgh, Edinburgh, UK
- ⁶⁰ School of Physics and Astronomy, University of Glasgow, Glasgow, UK
- ⁶¹ Oliver Lodge Laboratory, University of Liverpool, Liverpool, UK
- ⁶² Imperial College London, London, UK
- ⁶³ Department of Physics and Astronomy, University of Manchester, Manchester, UK
- ⁶⁴ Department of Physics, University of Oxford, Oxford, UK
- ⁶⁵ Massachusetts Institute of Technology, Cambridge, MA, USA
- ⁶⁶ University of Cincinnati, Cincinnati, OH, USA
- ⁶⁷ University of Maryland, College Park, MD, USA
- ⁶⁸ Los Alamos National Laboratory (LANL), Los Alamos, NM, USA
- ⁶⁹ Syracuse University, Syracuse, NY, USA
- ⁷⁰ Pontifícia Universidade Católica do Rio de Janeiro (PUC-Rio), Rio de Janeiro, Brazil, associated to ³
- ⁷¹ School of Physics and Electronics, Hunan University, Changsha, China, associated to ⁸
- ⁷² Guangdong Provincial Key Laboratory of Nuclear Science, Guangdong-Hong Kong Joint Laboratory of Quantum Matter, Institute of Quantum Matter, South China Normal University, Guangzhou, China, associated to ⁴
- ⁷³ Lanzhou University, Lanzhou, China, associated to ⁵
- ⁷⁴ School of Physics and Technology, Wuhan University, Wuhan, China, associated to ⁴
- ⁷⁵ Departamento de Física, Universidad Nacional de Colombia, Bogota, Colombia, associated to ¹⁶
- ⁷⁶ Ruhr Universitaet Bochum, Fakultae f. Physik und Astronomie, Bochum, Germany, associated to ¹⁹
- ⁷⁷ Eotvos Lorand University, Budapest, Hungary, associated to ⁴⁹
- ⁷⁸ Van Swinderen Institute, University of Groningen, Groningen, The Netherlands, associated to ³⁸
- ⁷⁹ Universiteit Maastricht, Maastricht, The Netherlands, associated to ³⁸
- ⁸⁰ Tadeusz Kosciuszko Cracow University of Technology, Cracow, Poland, associated to ⁴¹
- ⁸¹ Universidade da Coruña, A Coruña, Spain, associated to ⁴⁵
- ⁸² Department of Physics and Astronomy, Uppsala University, Uppsala, Sweden, associated to ⁶⁰
- ⁸³ Taras Schevchenko University of Kyiv, Faculty of Physics, Kyiv, Ukraine, associated to ¹⁴
- ⁸⁴ University of Michigan, Ann Arbor, MI, USA, associated to ⁶⁹
- ⁸⁵ Ohio State University, Columbus, USA, associated to ⁶⁸

^a Centro Federal de Educação Tecnológica Celso Suckow da Fonseca, Rio De Janeiro, Brazil

- ^b Center for High Energy Physics, Tsinghua University, Beijing, China
 - ^c Hangzhou Institute for Advanced Study, UCAS, Hangzhou, China
 - ^d School of Physics and Electronics, Henan University, Kaifeng, China
 - ^e LIP6, Sorbonne Université, Paris, France
 - ^f Lamarr Institute for Machine Learning and Artificial Intelligence, Dortmund, Germany
 - ^g Universidad Nacional Autónoma de Honduras, Tegucigalpa, Honduras
 - ^h Università di Bari, Bari, Italy
 - ⁱ Università di Bergamo, Bergamo, Italy
 - ^j Università di Bologna, Bologna, Italy
 - ^k Università di Cagliari, Cagliari, Italy
 - ^l Università di Ferrara, Ferrara, Italy
 - ^m Università di Genova, Genoa, Italy
 - ⁿ Università degli Studi di Milano, Milan, Italy
 - ^o Università degli Studi di Milano-Bicocca, Milan, Italy
 - ^p Università di Padova, Padua, Italy
 - ^q Università di Perugia, Perugia, Italy
 - ^r Scuola Normale Superiore, Pisa, Italy
 - ^s Università di Pisa, Pisa, Italy
 - ^t Università della Basilicata, Potenza, Italy
 - ^u Università di Roma Tor Vergata, Rome, Italy
 - ^v Università di Siena, Siena, Italy
 - ^w Università di Urbino, Urbino, Italy
 - ^x Universidad de Ingeniería y Tecnología (UTEC), Lima, Peru
 - ^y Universidad de Alcalá, Alcalá de Henares, Spain
 - ^z Facultad de Ciencias Físicas, Madrid, Spain
 - ^{aa} Department of Physics/Division of Particle Physics, Lund, Sweden
- *Deceased